

In presenting this dissertation/thesis as a partial fulfillment of the requirements for an advanced degree from Emory University, I agree that the Library of the University shall make it available for inspection and circulation in accordance with its regulations, governing materials of this type. I agree that permission to copy from, or to publish, this thesis/dissertation may be granted by the professor under whose direction it was written, or, in his/her absence, by the Dean of the Graduate School when such copying or publication is solely for scholarly purposes and does not involve potential financial gain. It is understood that any copying from, or publication of, this thesis/dissertation which involves potential financial gain will not be allowed without written permission.

Student's signature

Yuting Li

Influence of Arginine 355 and Glutamate 758 on the Substrate Specificities
and Catalytic Properties of *C. acidovorans* Xanthine Dehydrogenase

By

Yuting Li

Master of Science

Department of Chemistry

Dale E. Edmondson, Ph.D.
Adviser

Cora E. MacBeth, Ph.D.
Committee Member

Kurt Warncke, Ph.D.
Committee Member

Accepted:

Lisa A. Tedesco, Ph.D.
Dean of the Graduate School

Date

Influence of Arginine 355 and Glutamate 758 on the Substrate Specificities
and Catalytic Properties of *C. acidovorans* Xanthine Dehydrogenase

By

Yuting Li

M.S., Nanjing University, 2005

Adviser: Dale E. Edmondson, Ph.D.

An Abstract of

thesis submitted to the Faculty of the Graduate
School of Emory University in partial fulfillment
of the requirements for the degree of
Master of Science

Department of Chemistry

2007

Xanthine dehydrogenase (XDH) was engineered to an aldehyde-oxidizing enzyme (ADH) by a single amino acid mutation with the benefit of identifying the functional roles of active site amino acids in the related XDH and aldehyde oxidase (AO) enzymes that distinguish their respective catalytic activities. Arg355Met *C. acidovorans* XDH was expressed and purified using pUCP-Nde/*P. aeruginosa* expression system. Arg355Met XDH exhibits a similar UV-Vis spectrum and CD spectrum with those of the wild-type XDH. On comparison with wild-type enzyme, the mutant enzyme shows 0.4% of the k_{cat} with xanthine, and 3% with hypoxanthine. Interestingly, Arg355Met XDH shows catalytic activity with phenanthridine, which is a substrate of AO but not a substrate of XDH. These results suggest that the Arg355Met XDH has a similar active site structure to that of the wild-type XDH and that Arg355 plays an important role in catalysis of xanthine hydroxylation. The Arg355Met mutation results in the functional conversion of XDH to that of an aldehyde dehydrogenase.

Glu758Gln XDH mutant expressed from *P. aeruginosa* was purified. An imidazole gradient was used for elution from Ni-NTA column during purification to separate the endogenous XDH in *P. aeruginosa* from the expressed mutant enzyme, because the presence of endogenous XDH will interfere with the kinetic behavior of the expressed enzyme that exhibits a very low catalytic activity. The recombinant mutant enzyme exhibits UV-Vis and CD spectral properties very similar to the wild-type XDH, and kinetic characterization of the Glu758Gln XDH at pH 7.8 reveals only 0.002% of turnover number of the wild-type XDH. The result shows the importance of Glu758 in

the catalytic mechanism of xanthine hydroxylation. Combined with previous results from our lab, a catalytic mechanism was proposed with Glu758 as a general base to initiate the reaction by deprotonating the Mo-OH group.

Influence of Arginine 355 and Glutamate 758 on the Substrate Specificities
and Catalytic Properties of *C. acidovorans* Xanthine Dehydrogenase

By

Yuting Li

M.S., Nanjing University, 2005

Adviser: Dale E. Edmondson, Ph.D.

A thesis submitted to the Faculty of the Graduate
School of Emory University in partial fulfillment
of the requirements for the degree of
Master of Science

Department of Chemistry

2007

ACKNOWLEDGEMENTS

My first acknowledgement will go to my advisor Dr. Dale E. Edmondson for his scientific guidance, enthusiasm and patience in the past two years. Sincere thanks to my committee members, Dr. Cora E. MacBeth and Dr. Kurt Warncke for the time they dedicated to evaluate my research and their guidance. I also would like to thank members of Edmondson's lab: Dr Anup Upadhyay, Dr. Jin Wang, Milagros Aldeco, Betul Kacar and Erica Milczek for their support and help. Special thanks to Dr. Manuela Trani who tutored me when I first came to the lab, also for her friendship.

Finally I would like to thank my husband and my parents for their supports all the time.

Table of Contents

Chapter I General Introduction	1
1.1 Molybdenum Hydroxylases	1
1.2 Xanthine Oxidoreductases	2
1.2.1 Eukaryotic XOR and Prokaryotic XOR.....	3
1.2.2 XOR cofactors	4
1.2.2.1 Molybdenum Pyranopterin	5
1.2.2.2 Iron-sulfur centers.....	7
1.2.2.3 Flavin Adenine Dinucleotide (FAD)	8
1.2.3 Properties of XOR.....	9
1.2.3.1 UV-Vis and CD Spectral Properties	9
1.2.3.2 EPR spectroscopy	11
1.2.4 Kinetics Studies of XOR.....	13
1.2.4.1 Steady State Kinetics	13
1.2.4.2 Reductive Half-reaction.....	14
1.2.4.3 Oxidative Half-reaction	15
1.2.4.4 Electron Transfer in XOR.....	16
1.2.4.5 Proposed Catalytic Mechanism.....	16
1.2.5 Expression Systems	20
1.3 Aldehyde Oxidase.....	21
1.3.1 Reaction Mechanism of Aldehyde Oxidase.....	22

1.4 Dissertation Objectives	23
Chapter 2 Engineering of the <i>C. acidovorans</i> Xanthine Dehydrnase to a Molybdo-enzyme with Aldehyde Dehydrogenase Functional Properties	24
2.1 Introduction.....	24
2.2 Materials and Methods.....	30
2.2.1 Materials	30
2.2.2 Construction of Vector pMT801 for Arg355Met Expression	31
2.2.3 Expression and purification of recombinant Arg355Met XDH	32
2.2.4 Characterization of recombinant Arg355Met XDH	32
2.2.5 Determination of the product obtained by oxidation of phenanthridine by Arg355Met XDH	35
2.2.6 Determination of inhibition constant of phenanthridine for WT XDH	35
2.2.7 Kinetics analysis for reactions of NADH and 6-phenanthridone formation	35
2.3 Results.....	36
2.3.1 Expression and purification of recombinant Arg355Met in <i>P. aeruginosa</i> PAOI-LAC	36
2.3.2 Characterization of recombinant Arg355Met from <i>P. aeruginosa</i> PAO1- LAC	39
2.3.2.1 Chemical properties and Spectral properties of recombinant Arg355Met XDH	39
2.3.2.2 Kinetic parameters of recombinant Arg355Met XDH at pH 7.8.....	43

2.3.3 Determination of the product obtained by oxidation of phenanthridine through Arg355Met <i>C. acidovorans</i> XDH	44
2.3.4 Determination of Inhibition constant of phenanthridine for WT XDH	47
2.3.5 Kinetics analysis for reactions of NADH and 6-phenanthridone formation	48
2.4 Discussion	50
2.5 Conclusion and future work	54

Chapter 3 Investigation of the Catalytic Mechanism of *C. acidovorans* Xanthine

Dehydrogenase: Characterization and Kinetics Studies on the Glu758Gln Active-Site Mutant	56
3.1 Introduction	56
3.2 Materials and Methods	59
3.2.1 Materials	59
3.2.2 Expression and purification of recombinant Glu758Gln XDH	59
3.2.3 Characterization of recombinant Glu758Gln XDH	60
3.3 Results	62
3.3.1 Expression and purification of recombinant Glu758Gln in <i>P. aeruginosa</i> PAO1-LAC	62
3.3.2 Characterization of recombinant Glu758Gln from <i>P. aeruginosa</i> PAO1-LAC	66
3.3.2.1 Spectral properties of recombinant Glu758Gln XDH	66

3.3.2.2 Chemical properties and kinetic parameters of recombinant Glu758Gln at pH 7.8.....	68
3.4 Discussion.....	69
Chapter 4 General Summary	74
References.....	78

List of Schemes

Chapter 1

Scheme 1 Reactions catalyzed by XORs: Hydroxylation of hypoxanthine to xanthine and of xanthine to uric acid	3
Scheme 2 Diagram of the redox turnover in XORs	5
Scheme 3 Riboflavin biosynthesis in <i>E. coli</i>	9
Scheme 4 XOR catalytic mechanism proposed by Bray's group	18
Scheme 5 XOR catalytic mechanism proposed by Hille's group	20
Scheme 6 Reaction mechanism for the aldehyde oxidase group	22

Chapter 3

Scheme 1 Proposed mechanism for the reductive half reaction of <i>C. acidovorans</i> XDH	73
--	----

List of Tables

Chapter 2

Table 1 Typical reactions that XDH and AO catalyzes.....	28
Table 2 Purification steps for recombinant Arg355Met <i>C. acidovorans</i> XDH.....	37
Table 3 Comparison of the properties of Wild-type and Arg355Met <i>C. acidovorans</i> XDH	42

Chapter 3

Table 1 Purification steps for endogenous XDH in <i>P. aeruginosa</i>	62
Table 2 Comparison of the purification steps for recombinant WT and Glu758Gln <i>C.</i> <i>acidovorans</i> XDH.....	65
Table 3 Comparison of the properties of pure recombinant WT and Glu758Gln <i>C.</i> <i>acidovorans</i> XDH.....	69

List of Figures

Chapter 1

Figure 1 Crystal structure of <i>R. capsulatus</i> XDH.....	4
Figure 2 Structure of Molybdopterin cofactor.....	6
Figure 3 Structure of 2Fe-2S centers.....	7
Figure 4 UV-Vis (A) and CD spectra (B) for native <i>C. acidovorans</i> XDH:.....	10
Figure 5 EPR spectra for <i>C. acidovorans</i> XDH.....	13

Chapter 2

Figure 1 Comparison of protein sequences of XOR and AO.....	25
Figure 2 Residues in the active site of bovine aldehyde oxidase.....	29
Figure 3 Western blot analysis of recombinant Arg355Met XDH _{ABC}	38
Figure 4 Coomassie stained SDS-PAGE gel analysis of recombinant Arg355Met XDH _{ABC}	38
Figure 5 UV-Vis of recombinant Arg355Met XDH _{ABC} expressed in <i>P. aeruginosa</i>	40
Figure 6 Circular Dichroism of oxidized recombinant Arg355Met XDH expressed in <i>P.</i> <i>aeruginosa</i>	40
Figure 7 Changes in the UV-Vis spectra after adding Arg355Met XDH to phenanthridine solution and UV-Vis spectrum of 6-phenanthridone.....	45
Figure 8 TLC result on silica gel 60 plates for product, phenanthridine and 6- phenanthridone.....	46

Figure 9 Typical Lineweaver-Burk plots for inhibitory activity of phenanthridine on the oxidation of xanthine by <i>C. acidovorans</i> XDH and K_m changes with the inhibitor concentration.....	47
Figure 10 Kinetics analysis for reactions of NADH and phenanthridone formation	48

Chapter 3

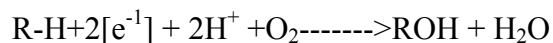
Figure 1 Active site of <i>R. capsulatus</i> XDH	58
Figure 2 Ni-NTA column chromatography of Glu758Gln <i>C.acidovorans</i> XDH	63
Figure 3 XDH activity in two peaks of endogenous XDH in <i>P. aerogenosa</i>	64
Figure 4 Characterization of Glu758Gln XDH. A) Western blot and B) SDS-PAGE	66
Figure 5 UV-Vis spectra of WT and Glu758Gln XDH	67
Figure 6 Circular Dichroism spectra of Glu758Gln XDH.....	68

Chapter 1

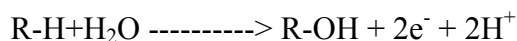
General Introduction

1.1 Molybdenum Hydroxylases

Hydroxylation reactions of aromatic or aliphatic carbon are ubiquitous in the metabolic pathways of living organisms, found in degradation of aromatic sources in bacteria and biosynthesis of neurotransmitters in eukaryotes. Monooxygenase systems in this group utilize O₂ as the ultimate source of the hydroxyl oxygen incorporated into product, including flavin-containing *p*-hydroxybenzoate hydroxylase and copper-containing dopamine-β-monooxygenase, heme-containing cytochromes P-450 and the non-heme iron-containing methane monooxygenase ^[1]. The reaction stoichiometry for monooxygenase systems is:



In contrast to monooxygenase systems, the molybdenum hydroxylases utilize H₂O as the ultimate source of the oxygen atom incorporated in the product^[2]. The reaction stoichiometry for molybdenum hydroxylases is:

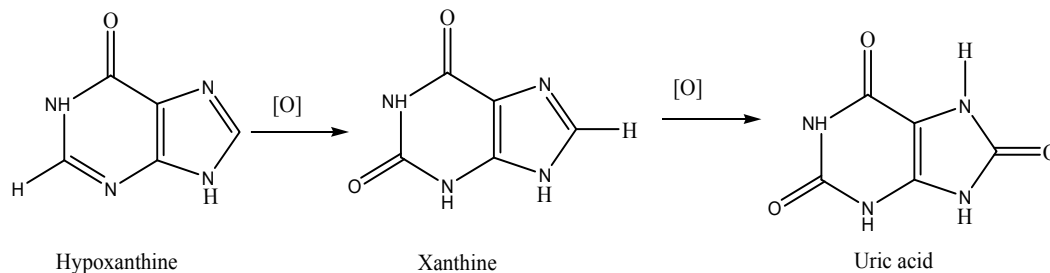


The family of Molybdenum Hydroxylases includes bacterial Nicotine Dehydrogenases, Nicotinic acid Hydroxylases, Formate Dehydrogenases, CO Oxidoreductases, eukaryotic Aldehyde oxidases, and eukaryotic and prokaryotic Xanthine Oxidoreductases. This family is divided into two classes based on the presence or absence of a terminal sulfide ligand on the molybdenum center. Xanthine

oxidoreductases and aldehyde oxidases belong to the former group that requires this sulfide ligand for their activity. Another distinguishing feature for xanthine oxidoreductases and aldehyde oxidases is the coordination of molybdenum by a single molybdopterin moiety, with no metal coordination by an amino acid side chain.

1.2 Xanthine Oxidoreductases

Xanthine Oxidase (XO, EC 1.2.3.2) and Xanthine dehydrogenase (XDH, EC 1.1.1.204) are two isoforms of the same molybdoflavoenzyme xanthine oxidoreductase that have been found in the cytosol of eukaryotic and prokaryotic organism. The function of XOR has been identified as catalyzing the last two steps in the degradation of purines: hydroxylation of hypoxanthine to form xanthine, and xanthine to form uric acid (Scheme 1). A high blood concentration of uric acid called hyperuricemia can cause gout and kidney and bladder stones^[3]. Products and byproducts of reduction of O₂ by XO are also well known oxidants, therefore XORs are also related to oxidative damage. Another medical condition related to XOR is xanthinuria, and xanthinuria types I, II, III are different forms of this disease^[4]. Type I is caused by XDH deficiency, while type II is caused by both XDH and AO deficiency. Xanthinuria type III has severe repercussions on the central nervous system leading to neurological disorders, which is caused by molybdenum cofactor deficiency^[5].



Scheme 1. Reactions catalyzed by XORs: Hydroxylation of hypoxanthine to xanthine and of xanthine to uric acid

The difference between XO and XDH is their different reactivities toward molecular oxygen and NAD^+ . O_2 is the electron acceptor of the redox cycle for XO, and NAD^+ is the acceptor for XDH. XDH can be converted to its oxidase form by either thiol oxidation (reversible) or by proteolytic modification (irreversible) [6].

1.2.1 Eukaryotic XOR and Prokaryotic XOR

Eukaryotic XOR has a homodimer α_2 structure, and each monomer contains a full complement of cofactors, with the total molecular weight around 150 kDa. In each active monomer, it has one Mo-pyranopterin active site (Moco), two [2Fe-2S] centers, and one FAD [7]. Prokaryotic XOR have been shown to have a more composite subunit organization [8]. Enzymes from *P. aeruginosa* [9], *C. acidovorans* [10], and *R. capsulatus* [11] show characteristics and spectral properties similar to the ones exhibited by eukaryotic XOR. Figure 1 shows the crystal structure of *R. capsulatus* XDH. These prokaryotic XORs are dimers of heterodimers $\alpha_2\beta_2$, and each α subunit (87 kDa for *C. acidovorans*) contains one Mo-pyranopterin active site (Moco), and each β subunit (58 kDa for *C. acidovorans*) contains one FAD and two iron-sulfur centers. The α subunit (XDHB) in *C. acidovorans* is encoded by *xdhB* gene, and the β subunit (XDHA) is

encoded by *xdhA* gene. A third gene, namely *xdhC*, which is co-transcribed with *xdhAB*, is required for XDH activity. However, it is not identified as a subunit of active XDH. XDH_C was proposed to be an XDH-specific Moco carrier protein, a Moco insertase or a chaperone involved in proper folding during or after the insertion of Moco into XDH^[12].

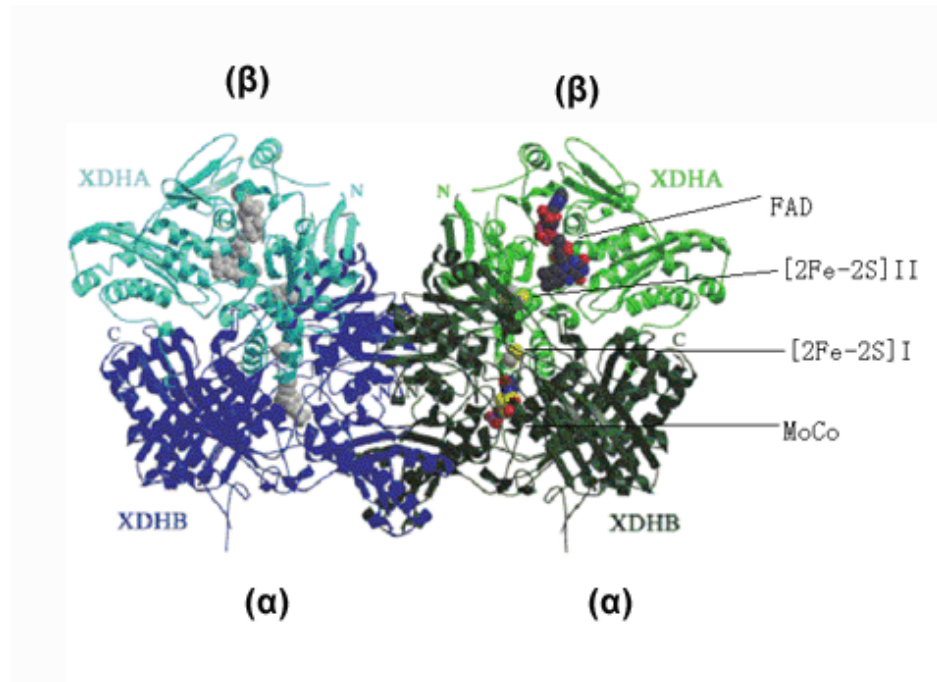
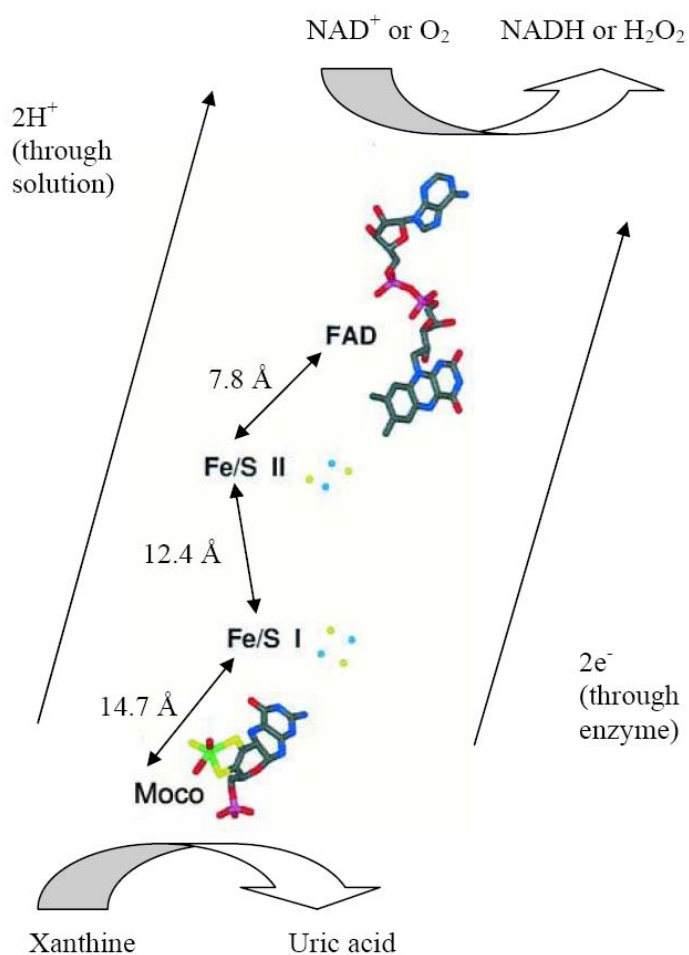


Figure 1. Crystal structure of *R. capsulatus* XDH^[11]. The notation used for *C. acidovorans* XDH subunits are in parentheses.

1.2.2 XOR Cofactors

Eukaryotic XOR and prokaryotic XOR from *P. aeruginosa*^[9], *C. acidovorans*^[10], and *R. capsulatus*^[11] all have four cofactors: molybdenum pyranopterin cofactor (Moco), two iron-sulfur centers and flavin adenine dinucleotide (FAD). The Moco active site is where oxidation of the substrate takes place and the FAD cofactor transfers the electrons to the final electron acceptor, either O₂ or NAD⁺. The two iron-sulfur centers function as electron transfer agents between these two sites. (Scheme 2)



Scheme 2 Diagram of the redox turnover in XORs, figure from bovine XO crystal structure ^[13]

1.2.2.1 Molybdenum Pyranopterin

In the substrate binding sites of XORs where the oxidation of xanthine to uric acid occurs, the molybdenum binds to a pyranopterin molecule (Figure 2). In oxidized XORs, Mo(VI) has a distorted squared pyramidal geometry. The apical position is occupied by a Mo=O group, which represents the strong-field ligand of the coordination sphere that defines the molecular z-axis of the center. The four equatorial ligands are a terminal Mo=S group, two sulfur atoms from the pterin cofactor via dithiolene bond, and

a hydroxyl group of a water molecule. XORs and aldehyde oxidase both require the terminal sulfur ligand for its activity, and the loss of Mo=S is the major cause of non-functional XOR both *in-vivo* and *in-vitro*, and it is known that Mo=S can be removed by treatment with cyanide to form thiocyanate, resulting in loss of activity ^[14]. The level of functional enzyme refers to XDH species containing a functional Mo catalytic Center ^[15]. The functionality of XDH, which represents the sulfured Mo content, is estimated as a ratio of change in the absorbance at 450 nm after anaerobic reduction of the enzyme with 1 mM xanthine relative to the absorption change after reduction by dithionite.

The pyranopterin cofactor is important in biology and 15 gene products are required for its biosynthesis. The metabolic pathway that leads to its biosynthesis can be divided into two parts: a first leading step from guanine and a C5 sugar to a metabolic intermediate-Precursor Z ^[16, 17], and a second step from this intermediate onto the mature cofactor. Study on *R. capsulatus* ^[18] and *C. acidovorans* ^[19] XDH have indicated that XDHC is involved in the Moco insertion process, but the details of mechanism of the insertion and intermolecular rearrangements are still unknown.

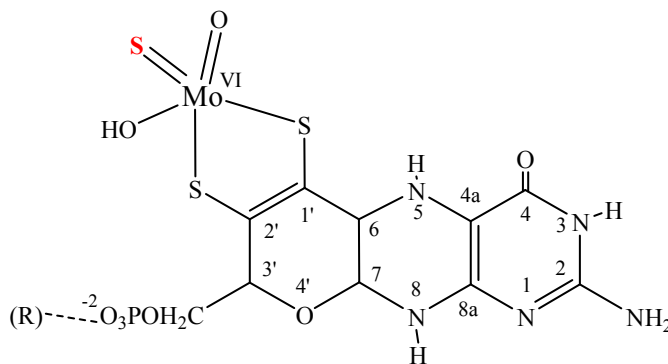


Figure 2. Structure of Molybdopterin cofactor

1.2.2.2 Iron-sulfur Centers

The iron-sulfur centers in XORs are [2Fe-2S] I and [2Fe-2S] II that function as the electron link between Moco active site and FAD cofactor. In these clusters, each Fe atom is coordinated by four sulfurs in a tetrahedral coordination, and two Fe atoms share bridging sulfurs (Figure 3). The other four ligands are four cysteine residues from the enzyme chain. The [2Fe-2S] I is about 14 Å from the Mo, and the [2Fe-2S] II is about 8 Å away from the flavin; the two clusters are separated by 12 Å. (scheme 2).

The first study on biosynthesis and post-translational formation of iron-sulfur clusters was performed on the nitrogen-fixing bacterium *Azotobacter vinelandii*. NifS and NifU, the gene product of nif operons, were shown to participate in iron-sulfur cluster formation. Further investigations on *E. coli* led to isolation of another operon *isc*, which consists of *iscSUA*, *hscB/hscA*, and *fdx* genes^[20]. The gene products of *iscU* homologous to N-terminal of NifU contains three conserved cysteine residues that form a labile mononuclear iron-binding site, and the study suggested that IscU functions as a template for assemble and transfer of [2Fe-2S] clusters to apoproteins. HscA and HscB function as two chaperons, helping maturation of the iron-sulfur centers^[21].

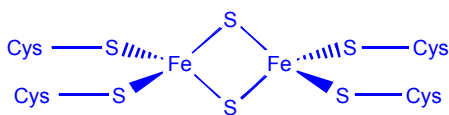
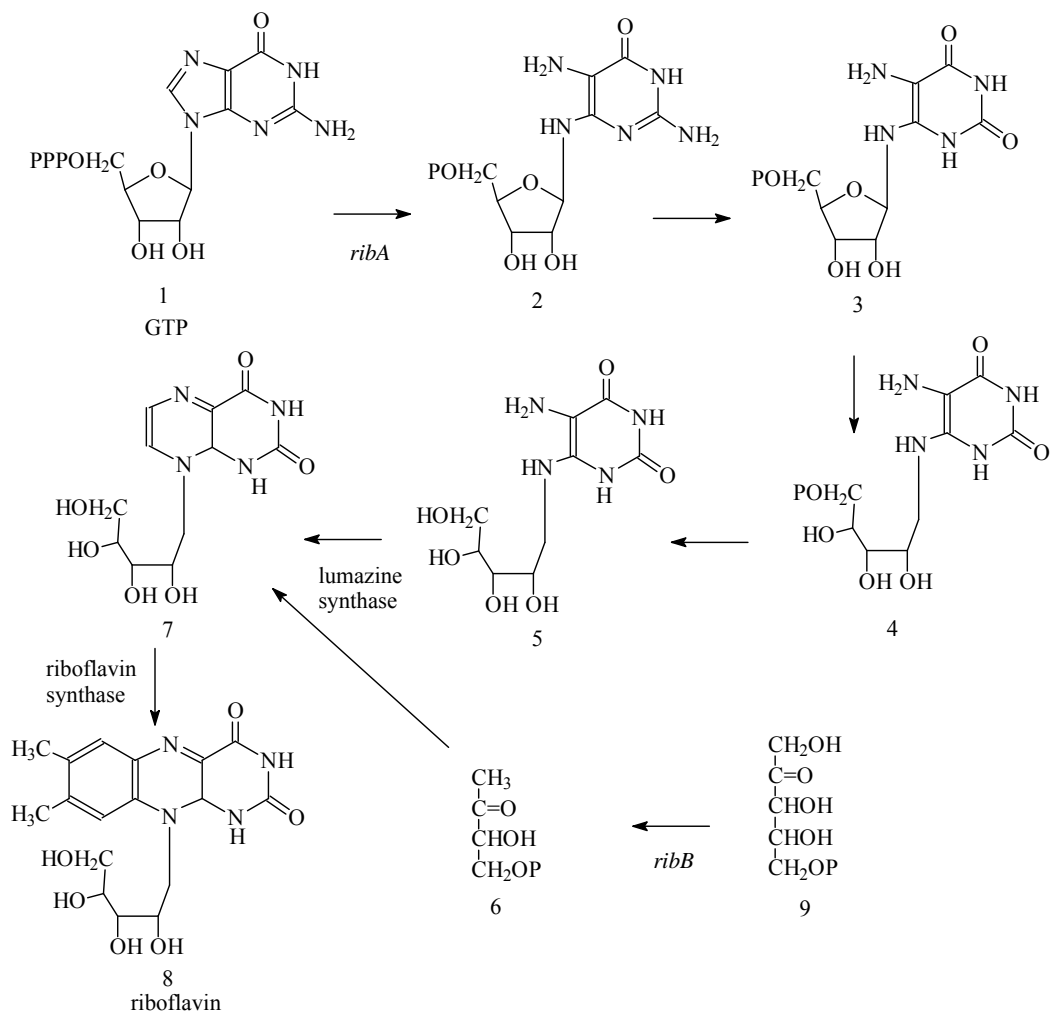


Figure 3 Structure of 2Fe-2S centers

1.2.2.3 Flavin Adenine Dinucleotide (FAD)

Flavins are widely found in many enzymes of both prokaryotic and eukaryotic organisms. In XORs, the function of FAD is to receive the electrons from xanthine oxidation and reduce NAD^+ in XDH or O_2 in XO. FAD is also the area of the XORs to undergo the conversion of XO and XDH: Four residues in milk XOR have been proved to be the “core” for the structural modification for XDH/XO conversion which results in narrowing the channel of access to the flavin [6].

Flavin Biosynthesis requires biosynthesis of riboflavin that in most cases can directly be synthesized by the organism [22]. Riboflavin biosynthesis has been studied in *E.coli*, *B. subtilis* and *S. cerevisiae*. Biosynthesis of riboflavin in *E. coli* comprises about seven steps, involved in several different enzymes (scheme 3). The biosynthesis of riboflavin starts with hydrolysis of GTP to GMP by GTP cyclohydrolase II. Then, the next two reactions involve the hydrolysis of the amino group (deaminase) and reduction of the ribosyl ring (reductase) and result in a compound 4. Compound 5 is fused with 3,4-dihydroxybutnone 4-phosphate and form compound 7 with the help of lumazine synthase after dephosphorylation. At the same time, the compound 6 is synthesized through a rearrangement of ribulose 5-phosphate by the 3, 4-dihydroxy-2-butanone-4-phosphate synthase. The procedure ends with the dismutation of two molecules of compound 7 catalyzed by riboflavin synthase and forming one molecule of riboflavin.



Scheme 3. Riboflavin biosynthesis in *E. coli*.

1.2.3 Properties of XOR

As previously mentioned, XOR from *P. aeruginosa* ^[9], *C. acidovorans* ^[10], and *R. capsulatus* ^[11] show similar characteristics and spectral properties to the ones as exhibited by eukaryotic XOR, which provided an efficient way to study eukaryotic XORs.

1.2.3.1 UV-Vis and CD Spectral Properties

As *B. Taurus* XO ^[8], the native *C. acidovorans* XDH shows the typical absorption band of the FAD at 370 nm and 450 nm, with the iron-sulfur centers bands with maxima

at 315 nm, 420 nm, and 467 nm in the UV-Vis spectrum ^[10] (Figure 4 (A)). The overlapping absorptions have a major peak at 462 nm, however, traditionally the XDH concentration is measured at 450 nm with extinction coefficient $\epsilon = 37,000 \text{ M}^{-1}\text{cm}^{-1}$.

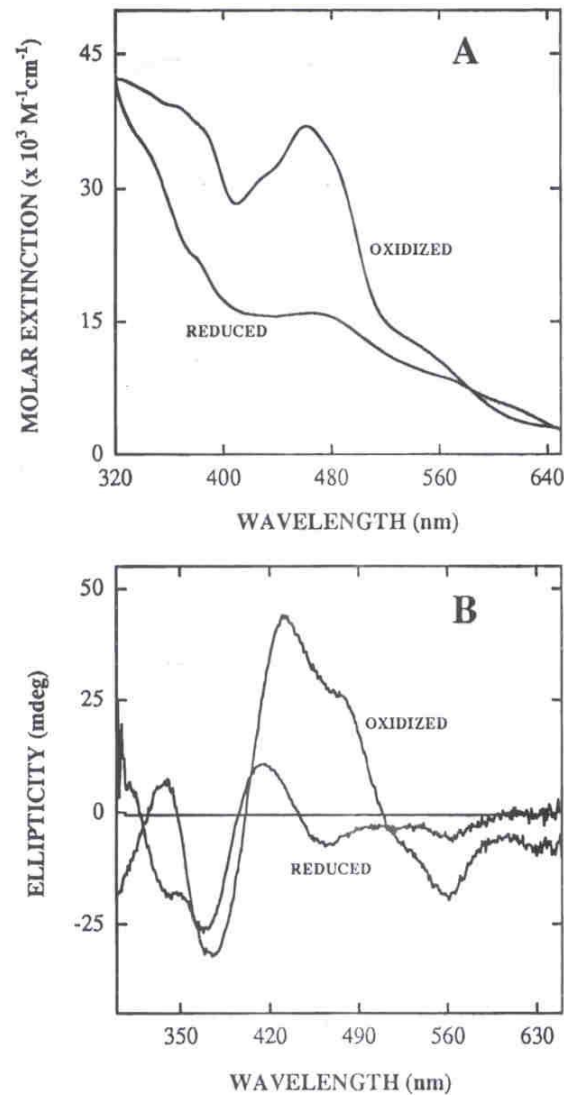


Figure 4. UV-Vis (A) and CD spectra (B) for native *C. acidovorans* XDH: oxidized (resting) and dithionite reduced enzyme ^[10]

The Circular Dichroism (CD) spectrum of native *C. acidovorans* XDH exhibits intense positive bands in the 400-500 nm region and strong negative bands in the 350-400 nm and in the 520-580 nm regions, which are a characteristic of oxidized [2Fe-2S]

centers as found in the milk XDH. The reduced forms of both XDHs show UV-Vis spectra and CD spectra a considerable reduction in intensities relative to the oxidized forms ^[10].

1.2.3.2 EPR Spectroscopy

EPR has been a primary method for elucidation of XORs mechanisms because the four cofactors create several paramagnetic species during reduction and re-oxidation procedures in the enzyme turnover. Resting XOR is EPR silent: Mo is diamagnetic d^0 Mo (VI), and the flavin is in its oxidized form. The 2 Fe (III) atoms (d^5 , spin 1/2 each) are antiferromagnetically coupled with each other and overall yield a diamagnetic species in iron-sulfur clusters. At 140 K, the EPR spectra of substrates and dithionite reduced *C. acidovorans* XDH shows the presence of the flavin radical with a typical isotropic radical signal of neutral semiquinone ($g=2.0$, peak to peak line width=2 mT), and of Mo (V) ($g_{av}=1.97$) trapped by rapid freeze quench technique ^[10] (Figure 5).

The earliest “very rapid Mo signal” is quite anisotropic and characterized by $g_1=2.0252$, $g_2=1.9550$, and $g_3=1.9494$. The signal exhibits little or no proton hyperfine coupling, and reduction with xanthine or 1-methylxanthine shows the maximal amount of this signal ^[23] which is not seen with all XO substrates.

Two types of “rapid” signal observed with XO at high and low xanthine concentrations, respectively. The “rapid” Type I signal, also detected with 1-methylxanthine, exhibits coupling to two inequivalent protons with $A_{ave}=1.3$ mT and 0.3 mT, and one of the two protons originates from the C-8 position in the xanthine molecule

and exchanges rapidly (27 s^{-1}) with the solvent ^[23, 24]. Type 1 is due to the formation of the catalytic intermediate. The second “rapid” Type 2 signal, which is also detected with 8-bromoxanthine, shows coupling to approximately two equivalent protons with $A_{ave}=1 \text{ mT}$, and type 2 is considered to come from the reduced form of the enzyme with an incorrectly oriented substrate.

The “slow” signal is attributed to slow reduction of desulfo Mo (V), which occurs by intermolecular transfer from active enzyme to inactive enzyme ^[25]. The signal is characterized as $g_1=1.9719$, $g_2=1.967$, $g_3=1.9551$, exhibiting coupling to two inequivalent protons as $A_{ave}=1.6 \text{ mT}$ for the strongly coupled proton and $A_{ave}=0.16 \text{ mT}$ for the weakly coupled proton. Treatment of desulfo XO with ethylene glycol produces the “desulfo-inhibited” Mo (V) signal.

The two [2Fe-2S] clusters can be distinguished by EPR. The [2Fe-2S] I shows signal with $g_1=2.022$, $g_2= 1.932$ and $g_3=1.894$ at high temperature (70 K), whereas [2Fe-2S] II is found with $g_1=2.110$, $g_2= 1.991$ and $g_3= 1.902$ below 25 K.

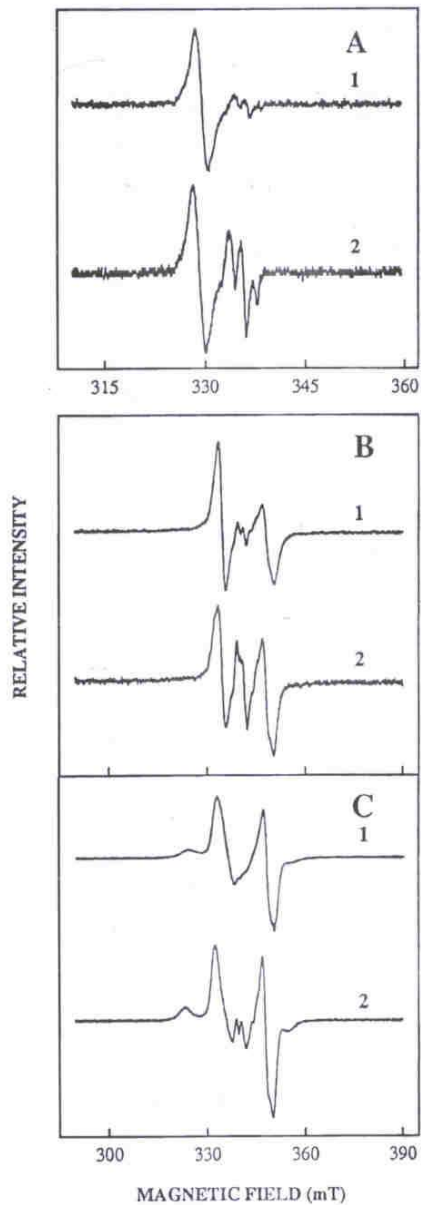


Figure 5. EPR spectra for *C. acidovorans* XDH. A) 140 K xanthine reduced (1) and dithionite reduced (2), B) 70 K xanthine reduced (1) and dithionite reduced (2), and C) 10 K xanthine reduced (1) and dithionite reduced (2) ^[10]

1.2.4 Kinetic Studies of XOR

1.2.4.1 Steady State Kinetics

As summarized in scheme 2, the reaction for XORs is that xanthine is oxidized to uric acid at the Moco active site, and through iron sulfur centers and the FAD cofactor

the electrons are finally transferred to electron acceptor, O_2 for XO and NAD^+ for XDH respectively. Conventional steady state kinetic studies on bovine XO [23] [7] and chicken and turkey XDH [26] [27] showed parallel lines in double reciprocal plots of kinetic data, which suggested a ping-pong mechanism for this reaction. Further crystal studies that demonstrated the distance between Moco active site and FAD confirmed this suggestion. The substrate inhibition occurs with excessive xanthine and saturating uric acid in XO [7], and similar results were found in chicken and turkey XDH [26, 28]. Lineweaver-Burk plots of $1/V_{max}$ vs. $1/[xanthine]$ on kinetic data of *C. acidovorans* XDH are non-parallel lines at high xanthine concentration [29].

1.2.4.2 Reductive Half-reaction

Three moles of xanthine and six moles of electrons are needed to reduce one mole of XORs: two electrons reduce Mo (VI) to Mo (IV), two electrons reduce two iron-sulfur centers (one for each), and finally two electrons reduce flavin. The reductive half-reaction of *B. taurus* XO includes a fast phase and a catalytically insignificant slow phase, which is due to intermolecular electron transfer between functional and non-functional forms of the enzyme [25]. However, for milk XO and turkey XDH, the reductive reaction might have fast XOR reduction to a four-electron state with the production as two moles of uric acid, followed by a slow rate reduction to a six-electron state that produces another mole of uric acid [26, 30]. For chicken and milk XDH, there are more complex three phases for the reduction process [30, 31]. For the chicken enzyme, the first phase is the formation of urate/ XO complex when the oxidation of the first mole of xanthine occurs. Then in the

second phase, the urate releases with the redistribution of the electrons, and the second mole of xanthine binds to the enzyme. Finally the second mole of urate releases, again with the redistribution of the electrons.

Substrate isotope effect studies on the reductive half-reaction of *B. Raurus* XO showed that the release of uric acid was the rate limiting step in the catalytic turnover^[32], and the bovine XO and chicken XDH also exhibit similar properties^[33]. The results of pH dependence studies on *B. Raurus* XO reveal a bell-shaped curve indicating a double ionization system for the reduction process. The pK_a of 7.4 obtained from the curve was assigned to xanthine, and the pK_a at 6.6 was assigned to either the Mo-SH group or the Mo-OH group^[32].

1.2.4.3 Oxidative Half-reaction

The oxidative half-reaction is the process of oxidation of a six-electron reduced form of the enzyme, which is different for XO and XDH because of the different electron acceptor at the FAD domain^[6]. The oxidative half-reaction for XO requires four moles of oxygen and results in two moles of H₂O₂ and two moles of O₂⁻, undergoing a biphasic oxidation process. During the first fast phase ($k_{cat}=60\text{ s}^{-1}$) the first two pair of electrons leaves the fully reduced enzyme to form hydrogen peroxide and one mole of superoxide anion is formed by transferring one electron to oxygen. However, during the next slow phase ($k_{cat}=10^4\text{ s}^{-1}$), the last electron forms the second mole of superoxide anion in a second order process, and the XO gets completely oxidized^[34, 35].

The oxidative half-reaction for chicken liver XDH by oxygen was shown to be triphasic with the formation of superoxide anion but no hydrogen peroxide^[36]. The low binding affinity of oxygen for XDH causes the superoxide anion to be a minor product for the catalytic reaction. However, oxidation of chicken XDH by NAD^+ , a better substrate for XDH than O_2 , is monophasic with the formation of a tight complex of the two-electron reduced enzyme with NADH ^[31].

1.2.4.4 Electron Transfer in XOR

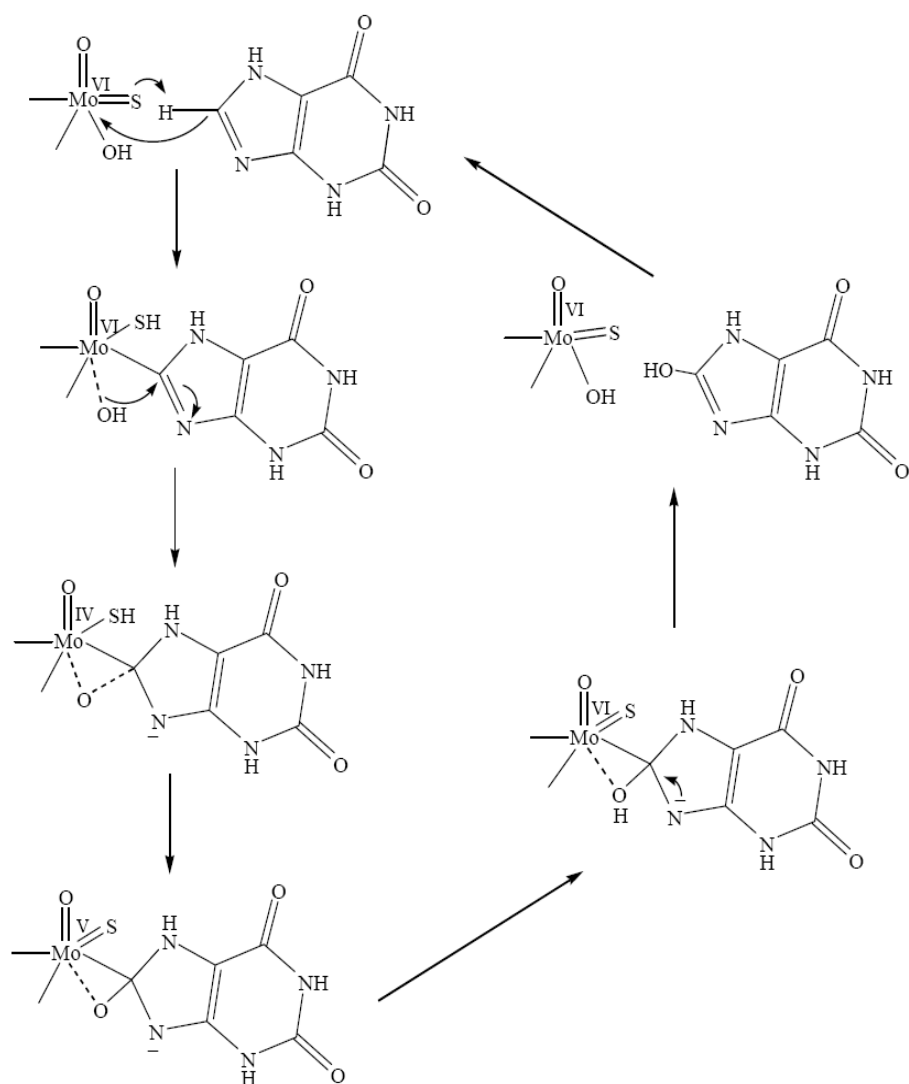
Investigation of the electron transfer rates for *B. taurus* XO and *G. gallus* XDH utilize some technique, such as flash photolysis ^[37], stop-flow pH jump technique ^[38] and pulse radiolysis ^[39]. The studies yielded similar results for both forms of the enzyme, suggesting that the transfer rate from Moco to FAD is significantly higher than the turnover rate of the enzyme and is not the limiting step of the reaction. For the rate of electron transfer from an iron-sulfur cluster I to the flavin, the rate of restoration of the equilibrium for partial reduced bovine XO measured by stopped-flow pH-jump technique was 173 s^{-1} , and 395 s^{-1} for the reverse rate. The rate of electron transfer from Moco to $[\text{2Fe-2S}]$ was measured as 8500 s^{-1} by pulse radiolysis analysis, and the rate of subsequent transfer to FAD is 150 s^{-1} . Furthermore, the electron transfer rate from Moco to FAD in chicken XDH is 1600 s^{-1} , as measured by laser flash photolysis.

1.2.4.5 Proposed Catalytic Mechanism

There are several catalytic mechanisms for the reaction of XOR with xanthine proposed in the last ten years, and the one proposed by Bray's group and the one by Hille's group are the most important two mechanisms.

The reaction mechanism proposed by Bray's group was based on EPR and ENDOR data of Mo(V) species which suggested to be formed when reoxidation of Mo(VI) to Mo(IV) occurs after the C-H is cleaved^[40]. The Mo-C distances were estimated in the inhibited (with formaldehyde and allopurinol) and "very rapid" Mo (V) EPR signals with substrate (xanthine) to be 1.9 Å and 2.4 Å. A strong coupling from ¹⁷O of a non-oxo group of oxidized enzyme appears in the uric acid product. Another work on model compounds^[41] indicated the contribution of Mo-O-C for the strongly coupled ¹⁷O in "very Rapid" Mo (V), and the work also showed "rapid Type One" Mo (V) coupling with the oxo group.

The mechanism from Bray's group is shown in Scheme 4. The C8 of xanthine adds to the Mo and the hydrogen transfers to the terminal S atom on the Mo. Then the hydroxyl group incorporates, and an intermediate forms, followed by loss of the H bound to the S and reduction of the Mo to generate the "very rapid" Mo (V) signal. The uric acid product is released upon reduction to Mo (IV), and then a new H₂O from the solvent bound to Mo to complete the turnover. The criticism of this mechanism is that most hypotheses are from EPR studies of the Mo (V) signal which is formed after the C-H cleavage step.

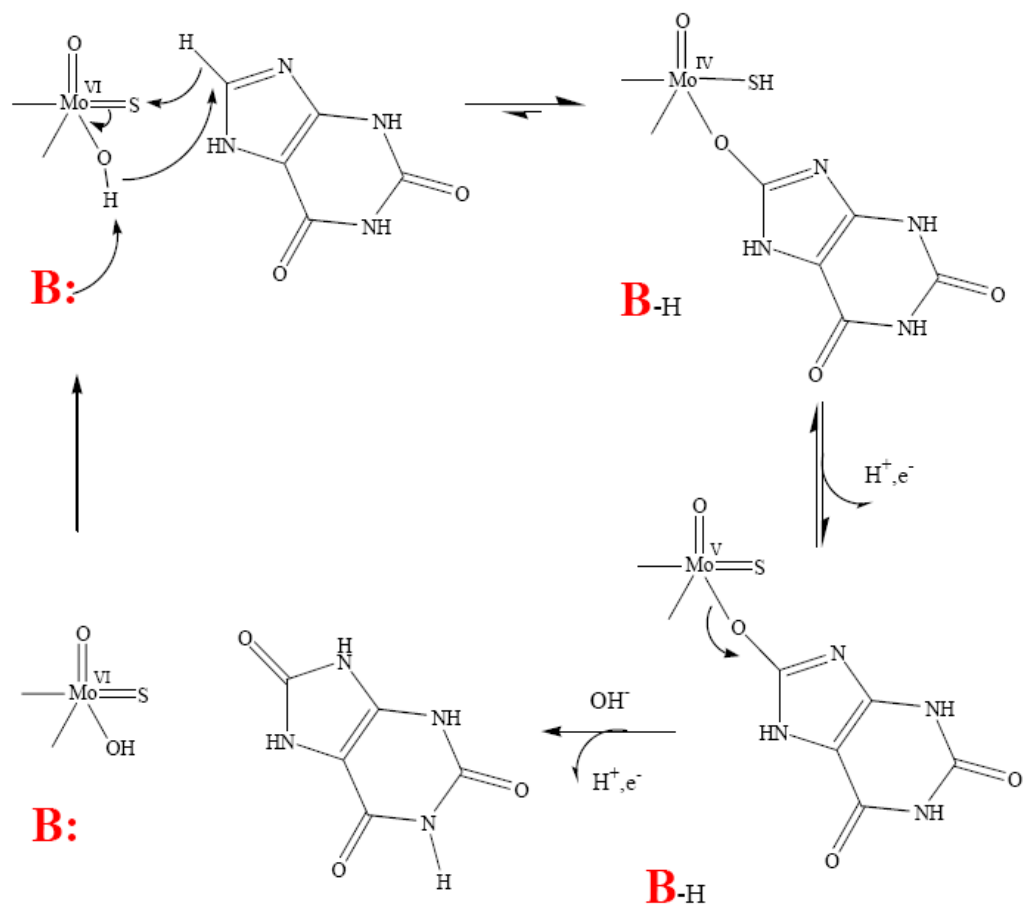


Scheme 4. XOR catalytic mechanism proposed by Bray's group ^[40]

The mechanism proposed by Hille's group was based on isotope effect, MASS spectral, and EPR studies ^[42]. The single turnover experiments with H_2^{16}O and H_2^{18}O show that there is a catalytically labile site on the enzyme that is the proximal donor of the oxygen atom incorporated into product, and EPR data showed that Mo-OH represent the catalytically labile site ^[1]. Freeze-quench EPR of deflavo xanthine oxidase showed the appearance and disappearance of "very rapid" Mo (V) correlate with the similar

results from UV-Vis stopped-flow experiments, and other “Rapid” Mo (V) signals were not present in single turnover experiments ^[43]. The result indicates that only Mo (V) “very rapid” signals are catalytically significant, and the two types of “rapid” Mo (V) found are thought to be substrate complex with no relevance with catalysis mechanism.

Scheme 5 shows the mechanism proposed by Hille’s group ^[42]. The active site base facilitates nucleophilic attack of the hydroxyl group of Mo to the C8 of xanthine to form an intermediate with Mo-O-C bond. Then internal electron transfer generates the “very rapid” Mo(V) signal after losing the H bound to the S, and further oxidation to Mo(VI) further releases the uric acid followed by the vacancy filled by a water molecule ^[42]. The presence of Mo-O-C is further proved by Raman and EXAFS studies ^[44, 45].



Scheme 5 XOR catalytic mechanism proposed by Hille's group ^[42]

1.2.5 Expression Systems

The studies of XOR have been limited to bovine xanthine oxidase for considerable period of time due to the ease of isolation of large quantities of XO from bovine milk. Heterologous expression of recombinant *R.norvegicus* XDH in a system consisting of baculovirus *Autographa californica* and insect cells of *Spodoptera frugiperda* produced very low expression yields ^[46]. Further expression of *D. melanogaster* XDH in *A. nidulans* ^[47] and homologous expression *D. melanogaster* XDH ^[48] both did not produce satisfactory yields level of enzyme in any of those systems.

Prokaryotic XORs from *C. acidovorans*, *P. aeruginosa* and *R. capsulatus* show similar characteristics and spectral properties to their eukaryotic counterparts. XDHs from these three organisms have pyranopterin in its monophosphate form in Moco site as the eukaryotic enzymes. The coexpression of *xdhc* is found to increase the amount of functionalized (sulfurated) Moco cofactor insertion in *E. coli* [18, 19]. The high level expression system was developed on expression *C. acidovorans* XDH in *P. aeruginosa* PAO1-LAC system, providing 56 mg of recombinant enzyme/L culture [15]. This system produced sufficient enzyme to permit complete kinetic and spectral studies on XDH for better understanding the mechanism both in prokaryotic and eukaryotic form.

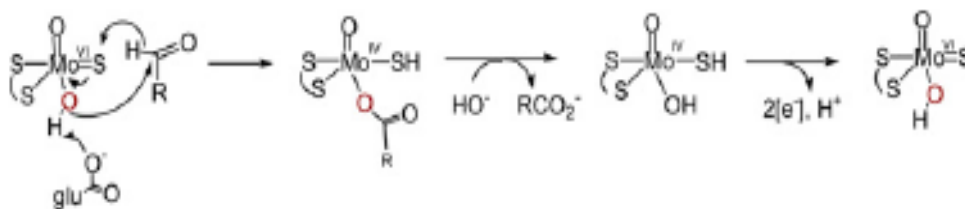
1.3 Aldehyde Oxidase

Aldehyde Oxidase (AO) is a cytoplasmic enzyme that catalyze the oxidation of a variety of aromatic and non-aromatic heterocycles and aldehydes, thereby converting them to the respective carboxylic acids or ketones [49]. AO enzymes are very similar to XDH enzymes as they share a high degree of sequence homology, have similar molecular mass, bind the same cofactors, and form dimmers. AOs are strict oxidases that use O₂ as electron acceptor and do not react with NAD⁺ as electron acceptor [50]. Animal AO, which is abundant in the liver and the lung, converts retinaldehyde into retinoic acid, the active metabolite of vitamin A [51, 52]. AO is also implicated in controlling the homeostasis of some types of tissues and hepatotoxicity of ethanol in mammals [53]. Plant AOs form a multigene family that can catalyze the final step in biosynthesis of the phytohormones ABA and auxins, namely IAA and 1-naphthalene acetic acid. Therefore,

in plants AO enzymes are essential for many physiological processes that require the involvement of the hormones abscisic acid and/or auxines. [54, 55]

1.3.1 Reaction Mechanism of Aldehyde Oxidase

In contrast to XDH, little is known about the catalytic mechanism of AO. Due to the high sequence and structural similarities between XDH and AO, the reaction mechanisms are commonly assumed to be very similar [8], and base-assisted catalysis has been demonstrated in the reaction of the bovine xanthine oxidoreductase with an aldehyde substrate [42]. The general mechanism of aldehyde oxidase is largely inferred from studies on XOR. The fact that Glu1261 in *B. taurus* XOR is strictly conserved suggests a similar mechanism as shown in Scheme 6. When the conversion of aldehydes to the corresponding carboxylic acid occurs in the hydroxylation of heterocycles, the nucleophilic bases attack the Mo-OH on the substrate carbonyl with concomitant hydride transfer [1]. The role for the glutamate had been proposed for the *D. gigas* aldehyde oxidoreductase [56].



Scheme 6 Reaction mechanism for the aldehyde oxidase group [1].

1.4 Dissertation Objectives

C. acidovorans XDH has been showing similar properties to those exhibited by the eukaryotic enzymes ^[10], and the high level expression system in *P. aeruginosa* provided a better way to study the mechanisms and catalytic characteristics of *C. acidovorans* XDH ^[15]. Based on this system, one goal for the dissertation is to investigate the role of Glu758 in the catalytic mechanism, and a mechanism is proposed, combined with the kinetics study on Glu277. Another goal of this dissertation is to engineer *C. acidovorans* XDH to a molybdoenzyme with aldehyde dehydrogenase functional properties. Based on the similarities of the residues in the active site of XDH and AO, through the single amino acid mutations of Arg355 in the active site of *C. acidovorans* XDH, the catalytic functions with different substrates are investigated. Comparison of the kinetics results will provide a further insight in the catalytic mechanism for both XORs and AO.

Chapter 2

Engineering of the *C. acidovorans* Xanthine Dehydrogenase to a Molybdo-enzyme with Aldehyde Dehydrogenase Functional Properties

2.1 Introduction

Site-directed mutagenesis has made it possible for function change of an enzyme, due to the development of biotechnology and bioinformatics^[57, 58]. These kinds of functional changes result in altered enantioselectivity, substrate selectivity, activity and thermal stability^[58, 59]. By making amino acid changes, the function of an enzyme can be altered to that of another enzyme^{[58] [60]}, and this transformation mostly occurs between enzymes in a super family that are related both in structure and biological function and provides the insight into mechanism of catalysis^[60]. Two amino acid replacements caused the substrate preference change from *Mig. Mthl* to MutY in the HhH superfamily. More interestingly, a number of studies have shown that single mutations can convert the function of enzymes. By making one amino acid change, the function of arylmalomate decarboxylase has been converted to that of a racemase^[58].

The molybdo-flavoenzymes (MFEs) are a subgroup of molybdo-proteins that require both Moco and a flavin cofactor for their catalytic activities, present in bacterial, fungal, plant and animals^[61]. The reductive half-reaction of substrate hydroxylation occurs on molybdopterin monophosphate cofactor (Moco) and the oxidative half-reaction of NAD⁺ or dioxygen reduction happens with participation of FAD cofactor. MFEs are a group of structurally and biochemically related proteins, and there are two main members

in this group: xanthine oxidoreductase [xanthine dehydrogenase(XDH) form, (EC1.1.1.204) and xanthine oxidase(XO) form EC 1.1.3.22] and aldehyde oxidase.(EC 1.2.3.1) ^[61]. The biochemical and physiological functions of aldehyde oxidase are largely obscure, while those of xanthine oxidase are widely recognized and investigated.

Aldehyde oxidases(AO) and xanthine dehydrogenases are very close in terms of not only general structure, cofactor content and biochemical characteristics, but also their sequences, mechanism of action and many other properties ^[61]. AO and XDH have nearly identical molecular mass, both have Moco, FAD, and Iron cofactors, and both form dimers. The overall similarity level in gene sequences between AO and XDH is around 50% ^[61-63] (Figure 1), and it was already shown by phylogenetic analysis that AO proteins have been derived from XDH by ancient gene duplications ^[64, 65]. In addition, due to the high sequence and structural similarities, the reaction mechanisms are commonly assumed to be very similar ^[8].

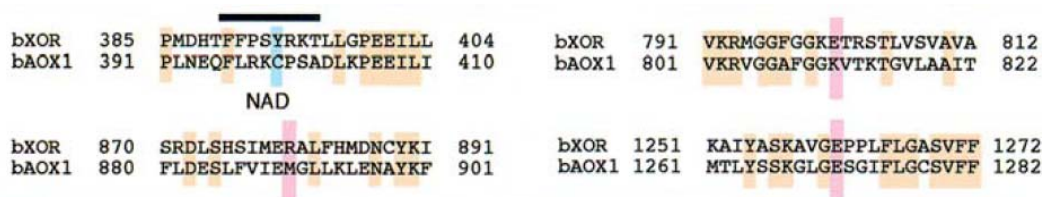


Figure 1^[61]. Comparison of protein sequences of XOR and AO. Identical and similar amino acids in the two sequences are boxed in yellow and grey respectively. The position of the sequence corresponding to the conserved NAD⁺-binding site identified in chicken XOR is indicated by a thick solid line above the two sequences. Amino acid residues involved in the binding of the substrate at the molybdenum center are boxed in pink ^[61].

However, XDH and AO have quite different substrate specificities for catalysis. In particular, aldehyde oxidase is unable to oxidized xanthine or hypoxanthine. Table 1

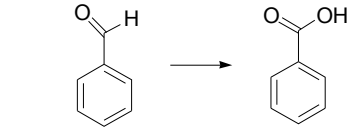
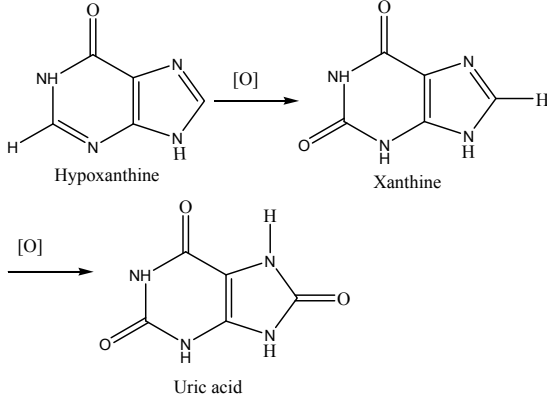
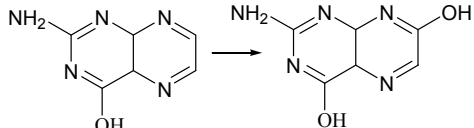
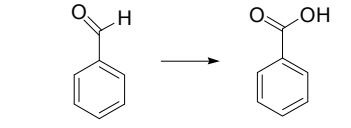
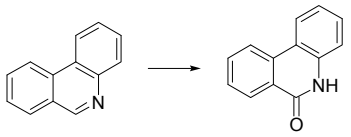
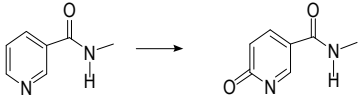
summarizes the typical reactions that XDH and AO catalyzes separately. AO can oxidize aromatic azaheterocycles containing $-\text{CH}=\text{N}-$ chemical function, aromatic or non-aromatic charged azaheterocycles with a $-\text{CH}=\text{N}^+$ -moiety (e.g. N-methylnicotinamide) or aldehydes (e.g. benzaldehyde) ^[66]. Some of the AO substrates are common to XDH, however, the specificity differences between the AO and XDH are the effects of the number and position of the ring substituents ^[67].

The different substrate specificities for AO and XDH were likely dictated by factors, such as protonation state of the MoCo and amino acid variations at the enzyme active sites of AO and XOR ^[68] ^[69]. A recent study was performed by using density functional calculations to predict the regioselectivity of drugs and molecules metabolized by AO and examining the energies of likely tetrahedral intermediates resulting from nucleophilic attack on the carbon being hydroxylated ^[70]. The study showed the energy of the tetrahedral intermediates is predictive for AO, but not for XOR, which indicates the oxidation of substrates by AO is due primarily to the electronic effects on the substituent, with AO playing very little role in orientation. Specific hydrogen bonds to the nitrogen adjacent to the electrophilic carbon on the substrate in the case of XOR probably account for the failure of the method to predict the energetics of the hydroxylation reaction.

The crystal structure of bovine XDH/XO with bound salicylate and the crystal structure of *R. capsulatus* XDH with bound alloxanthine reveals the residues of the active site potentially participating in the catalytic mechanism ^[13] ^[71]. XDH and AO have

similar structures and sequences, but differ in substrate specificity and activity, which may account for different residues around active site. Figure 2 presents the residues in the active site of bovine aldehyde oxidase as modeled by homology to the structure of bovine XDH. Some of these residues are the same for both enzymes, but there are several positions occupied by different residues for AO and XDH which might account for differing activities and substrate specificities. Arg880 in bovine XDH, which is a equivalent residue of Arg355 in *C.acidovorans*, is conserved in all xanthine oxidoreductases, but not in AO ^[51]. This residue may be important for the positioning of purine substrates in the Mo active site, which is supported by the point mutations of the corresponding Arg residue to either Gln or to Gly in *Aspergillus nidulans* XOR resulting in changing the hydroxylation position of the 2-hydroxypurine ring from C8 to C6 ^[72].

Table 1 Typical reactions that XDH and AO catalyzes

Reactions catalyzed by XDH ^[73]	Reaction catalyzed by AO
<p>1) benzaldehyde</p>  <p>benzaldehyde benzoic acid</p> <p>2) Purines</p>  <p>Hypoxanthine Xanthine</p> <p>Uric acid</p> <p>3) Pteridines</p>  <p>2-Amino-4-Hydroxy-Pteridine Isoxanthopterin</p>	<p>(1) benzaldehyde</p>  <p>benzaldehyde benzoic acid</p> <p>(2) phenanthridine</p>  <p>Phenanthridine 6-phenanthridone</p> <p>(3) N-Methylnicotinamide</p>  <p>N-Methylnicotinamide N-methyl-2-pyridone-5-carboxamide</p>

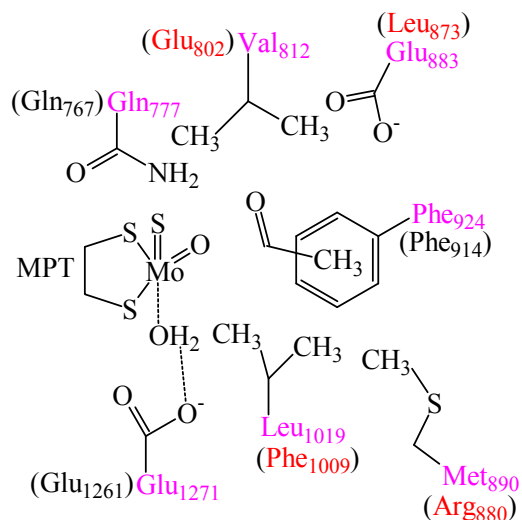


Figure 2. Residues in the active site of bovine aldehyde oxidase as modeled by homology to bovine XDH. The O=CH-CH₃ is the substrate acetaldehyde.

Moreover, according to computational analysis of xanthine dehydrogenase active sites by the LPC program and the DiverScan program based on the crystal structure and gene sequences, a list of residues are provided that are predicted to be functionally diverged, that is, residues that are important for function in both enzymes and conserved within one functionality but different from a conserved residue in the other functionality [74]. Arg355 in *C. acidovorans* XDH is one of those residues that directly affects the binding of the substrate (xanthine) in XDH, and is predicted by the DiverScan program as a mutation point to convert the function of xanthine dehydrogenase to that of an aldehyde oxidoreductase.

Therefore, we chose Arg355 in *C. acidovorans* XDH for site-directed mutagenesis to Met to test their predictions since it is present at the corresponding position in aldehyde oxidase. Since we change only the residue in the Mo active site and change nothing in FAD factor, the mutant enzyme is still a dehydrogenase, not an

oxidase. Our purpose is to engineer XDH to an aldehyde dehydrogenase (ADH) and answer the question of how this mutation alters the catalytic properties and substrate specificity of the XDH.

XDH is a well studied enzyme, but many aspects of AO are quite obscure. This research might provide new insights of the mechanisms for the two enzymes, and to better understand these mechanisms which will enable the design of more effective inhibitors that can treat diseases related to XDH and AO.

2.2 Materials and Methods

2.2.1 Materials

QuikChange Site-Directed mutagenesis kit was purchased from Stratagene. Primers were ordered from Operon, Inc. and were HPLC purified. T4 ligase and restriction endonucleases were purchased from Promega (Madison, WI). The *E. coli*/*P. aeruginosa* shuttle vector pUCP-Nde and *P. aeruginosa* PAO1-LAC were generous gifts from Drs. Cronin and McIntire (Department of Veterans Affairs Medical Center, San Francisco, CA) ^[75]. *P. aeruginosa* PAO1-LAC was used as an expression host and was maintained on Luria-Bertani plates supplemented with 15 g/mL tetracycline^[76]. *E. coli* XL-10-Gold (Stratagene Inc.) was used as cloning hosts. DNA sequencing was performed by the Emory University Microchemical Facility. Broad range prestained SDS-PAGE molecular weight standards were obtained from Bio-Rad Laboratories (Hercules, CA). Ni-NTA resin was from Qiagen. All other reagents were purchased from

either Sigma-Aldrich Co. (St. Louis, MO), Fisher Scientific Co. (Pittsburgh, PA), or Denville Scientific (New Jersey).

2.2.2 Construction of Vectors pMT812 and pMT801 for Arg355Met Expression

Residues Arg355 was selected for mutagenesis on the basis of multiple alignment of 27 enzymes of the Xanthine Oxidase family by using and comparing results obtained with DiverScan and Diverge programs.^[74]

Mutagenesis was performed on pNI800 plasmid obtained by inserting the *xdhB* gene from the pNI459 construct^[15] at *NotI/SalI* restriction sites of pGEN5Zf(+) vector. The Forward primer used to obtain pNI803 was GCGCCGGTGATGACGATGGCGCTGTGCCATTTCGAC, and the reverse primer was the reverse complementation of the forward primers. The PCR cycle was designed on the basis of the QuickChange kit manual as follows: 2.5 min at 98 °C; 18 cycles: 30 sec at 98 °C, 1 min at 50 °C, 12 min at 68 °C. The reaction mixture was separated from the top oil layer by pipetting the bottom layer out. Then it was incubated for exactly 1 hour with *DPMI* for digestion. An aliquot (5µl) of the reaction was used in transformation of XL-10 chemically competent cell. Mutant *xdhB* was reinserted in the *NotI/SalI* restriction site of a fresh batch of pNI459 construct to yield the mutated pNI803 vector. *XdhC* gene was cut from the pNI807 construct^[15] and ligated into the *HindIII/BamHI* restriction sites of pNI803 vectors to obtain the final pYL803 constructs. pYL803 vector was transformed in XL-10 Gold chemically competent cells and re-sequenced to verify the presence of the

mutation. Finally the correct pYL803 vector was electroporated to *P. aeruginosa* PAO1-LAC for the expression of mutant forms of *C. acidovorans* XDH. A polyhistidine tag was added to the N-terminus end of the β subunit to facilitate purification of recombinant enzymes. The recombinant mutant XDH produced by strains pYL803 will be further referred to as Arg355Met.

2.2.3 Expression and purification of recombinant Arg355Met XDH

P. aeruginosa strains, pYL803 for Arg355Met, was grown as previously reported^[15]. Cells harvesting, breakage and enzyme purification schemes were also the same as previously described for the wild-type enzyme.^[15]

2.2.4 Characterization of recombinant Arg355Met XDH

UV-Vis absorption spectra were measured either on Lambda 2 spectrometer (Perkin-Elmer, Boston, MA) or a Cary 50 UV-VIS spectrophotometer (Varian Inc., Walnut Creek, CA) at 25 °C. Circular dichroism (CD) spectra were recorded from an average of six to eight scans on an AVIV model 62SD CD spectrometer at 25 °C using anaerobic quartz cuvettes.

XDH activity with xanthine substrate was measured by following the appearance of uric acid at 295nm ($\epsilon_{295}=9600 \text{ M}^{-1} \text{ cm}^{-1}$) at 25 °C in TE buffer (100 mM Tris-HCl, 1 mM EDTA, pH 7.8) with the addition of freshly prepared 15 mM xanthine and 50 mM NAD^+ to a final concentration of 0.6 mM xanthine and 2 mM NAD^+ respectively. One unit of enzyme activity is defined as the amount of enzyme required to produce 1 μmol of uric acid in one minute at 25 °C. Kinetic properties at pH 7.8 were measured on a

Lambda 2 spectrometer (Perkin-Elmer) at 25 °C in TE buffer (100 mM Tris, 1 mM EDTA, pH 7.8) using xanthine concentrations ranging between 15 μM and 900 μM and NAD^+ concentrations between 25 μM and 3000 μM . XDH activity with benzaldehyde / purine / hypoxanthine were measured by following the appearance of NADH at 340 nm ($\epsilon_{340}=6200 \text{ M}^{-1} \text{ cm}^{-1}$) at 25 °C in TE buffer (100 mM Tris-HCl, 1 mM EDTA, pH 7.8). Kinetic properties at pH 7.8 for benzaldehyde / purine / hypoxanthine were measured on Lambda 2 spectrometer (Perkin-Elmer) at 25 °C in TE buffer (100 mM Tris, 1 mM EDTA, pH 7.8) using benzaldehyde / purine / hypoxanthine concentrations ranging between 150 μM and 24000 μM , 150 μM and 3000 μM , 7.5 μM and 1200 μM , respectively, with rates followed by the rate of NADH formation. Steady state kinetic parameters were calculated for xanthine and NAD^+ by non linear fitting of data to the Michaelis-Menten equation using Origin 7.0.

ADH activity by oxidation of phenanthridine by Arg355Met was measured by following the appearance of NADH at 340nm ($\epsilon_{340}=6200 \text{ M}^{-1} \text{ cm}^{-1}$) at 25 °C in TE buffer. (100 mM Tris-HCl, 1 mM EDTA, pH 7.8) with the addition of freshly prepared 15 mM phenanthridine and 50 mM NAD^+ to a final concentration of 0.6 mM phenanthridine and 2 mM NAD^+ . One unit of enzyme activity is defined as the amount of enzyme required to produce 1 μmol of NADH in one minute at 25 °C. Kinetic properties at pH 7.8 were measured on Lambda 2 spectrometer (Perkin-Elmer) at 25 °C in TE buffer (100 mM Tris, 1 mM EDTA, pH 7.8) using phenanthridine concentrations ranging between 4.5 and 450

μM and NAD^+ concentrations between and 25 and 2000 μM . Kinetic properties at pH 7.8 were measured on Lambda 2 spectrometer (Perkin-Elmer) at 25 °C in TE buffer (100 mM Tris, 1 mM EDTA, pH 7.8) using benzaldehyde / purine / hypoxanthine concentrations ranging between 75 μM and 24000 μM , 7.5 μM and 1200 μM , 3000 μM and 9000 μM , separately. Steady state kinetic parameters were calculated for benzaldehyde and purine by non linear fitting to the Michaelis Menten equation using Origin 7.0, and for hypoxanthine they were calculated by linear fitting to Linweaver-Burk plots using Origin 7.0

The Biuret assay ^[77] was used to estimate protein concentrations in cell extracts and after the first purification step. Concentrations of enzymes from later purification steps and purified enzyme were determined spectrophotometrically at 450 nm ($\epsilon_{450} = 37,000 \text{ M}^{-1} \text{ cm}^{-1}$).

SDS-PAGE gels 7.5% were prepared according to Laemmli ^[78]. Western blot detection was performed using rabbit polyclonal antisera raised against purified *C. acidovorans* XDH ^[10] in a 1:2000 dilution and goat anti-rabbit IgG Alkaline Phosphatase conjugate (Sigma Co.) in 1:3000 dilution. Alkaline phosphatase substrate Sigma Fast BCIP/NBT tablets were used for visualization.

Metal analyses on the pure enzymes were performed with a Jarrell-Ash 965 ICP Plasma Emission Spectrometer at the Chemical Analysis Facility at University of Georgia in Athens, GA.

Functionality (level of sulfurated Moco) in wild-type and mutant enzymes were measured on 30 μM solutions by analytical determination of the amount of SCN^- released by the enzymes upon treatment with CN^- according to the method described by Sorbo. ^[79]

2.2. Determination of the product obtained by oxidation of phenanthridine by Arg355Met XDH

Uv-Vis spectra of time course of oxidation of phenanthridine by Arg355Met XDH were measured by Cary 50 UV-VIS spectrophotometer (Varian Inc., Walnut Creek, CA) at 25 °C. The interval between spectra accumulated was 20 mins.

Thin Layer Chromatography (TLC) was performed on silica gel 60 plates using EtOAc : Hexane = 25 : 75 (v/v) as developing solvent.

2.2.6 Determination of inhibition constant of phenanthridine for WT XDH

The inhibition constant of phenanthridine for WT XDH with xanthine as substrate was measured by following the appearance of NADH at 340nm ($\epsilon_{340}=6200 \text{ M}^{-1} \text{ cm}^{-1}$) at 25 °C in TE buffer (100 mM Tris-HCl, 1 mM EDTA, pH 7.8) with the xanthine concentration ranging between 15 μM and 600-900 μM and the phenanthridine concentrations as 0 μM , 150 μM , 300 μM and 450 μM and 600 μM . Steady state kinetic parameters were calculated by non linear fitting to the Michaelis-Menten equation using Origin 7.0

2.2.7 Kinetics analysis for reactions of NADH and 6-phenanthridone formation

The kinetics analysis for reactions of NADH and 6-phenanthridone formation were performed by measuring the phenanthridine kinetics at the concentration of NAD⁺ as 25 μM, 50 μM, 100 μM, 200 μM, respectively. Kinetic parameters at pH 7.8 were measured on Lambda 2 spectrometer (Perkin-Elmer) at 25 °C in TE buffer (100 mM Tris, 1 mM EDTA, pH 7.8) using phenanthridine concentrations ranging between 4.5 to 450 μM.

2.3 Results

2.3.1 Expression and purification of recombinant Arg355Met in *P. aeruginosa*

PAO1-LAC

Arg355Met was expressed and purified in pUCP-Nde /*P. aeruginosa* PAO1-LAC expression system, following the same procedure used to express and purify the WT recombinant enzyme. As in the WT enzyme, the mutant was His-tagged at the N-terminus of the β subunit to allow purification with metal affinity chromatography. This expression system is very efficient for the expression of mutant forms of *C. acidovorans* XDH. Table 2 summarizes purification steps and enzyme yields for the preparation of Arg355Met with different substrates. The amount obtained of the Arg355Met mutant (11.8 mg/L after Ni-NTA) is comparable to that obtainable for the wild-type recombinant enzyme (11.9 mg/L after Ni-NAT) ^[15]. Specific activities measured at each step of the purification with xanthine as the substrate show a pronounced difference between WT and mutant forms of XDH. The Arg355Met mutant exhibits only 0.048% of the activity

of the WT enzyme. Besides xanthine, the Arg355Met XDH exhibits activity with phenanthridine, which is a substrate for AO, not XDH.

The Arg355Met XDH exhibits positive cross-reactivity against *C. acidovorans* XDH antisera as shown by the Western Blot (Figure 2). SDS-PAGE (Figure 3) shows that Arg355Met XDH was obtained a reasonable pure form, and the purity is confirmed by the A_{280}/A_{450} ratio, which equals to 6.17. The purification result shows that the pUCP-Nde/*P. aeruginosa* expression system allows the expression of Arg355Met XDH in high yields and high purity, which is attributed to the coexpression of *xdhC* from *P. aeruginosa*.

Table 2 Purification steps for recombinant Arg355Met *C. acidovorans* XDH.^a

	Total protein (mg)	Phenanthridine as substrate			Xanthine as substrate		
		Specific activity (U/mg)	Total Activity (U)	Yield (%)	Specific activity (U/mg)	Total Activity (U)	Yield (%)
Crude extract	481.0 ^b	0.0056	26.95	100	0.0012	6.05	100
DE-52 column	76.0 ^b	0.0072	5.5	20.5	0.0066	5	82.6
Ni-NTA column	11.8 ^c	0.032	3.8	14.1	0.032	3.7	62.1

a Recalculated for 1 L of culture.

b Based of Biuret assay.

c Based on A_{450} and $\epsilon_{450} = 37,000 \text{ M}^{-1}\text{cm}^{-1}$

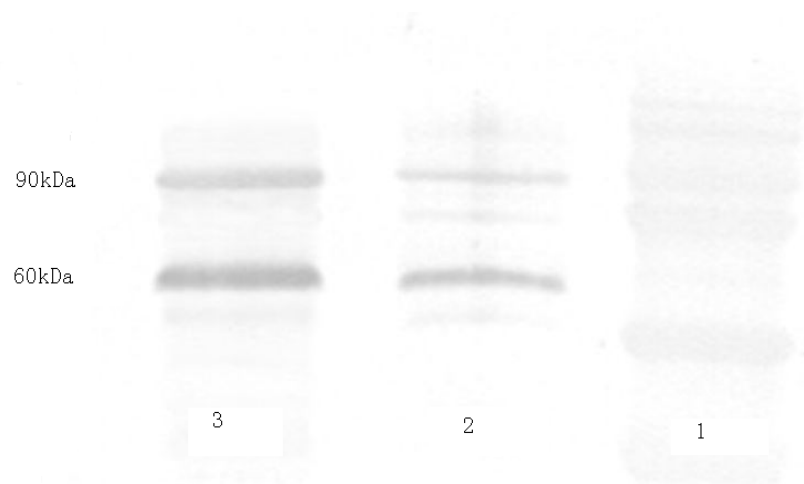


Figure 3. Western blot analysis of recombinant Arg355Met XDH_{ABC}. Lane 1: Molecular Weight Standards Lane 2: Arg355MetXDH_{ABC} Lane 3: Wild-type XDH_{ABC}

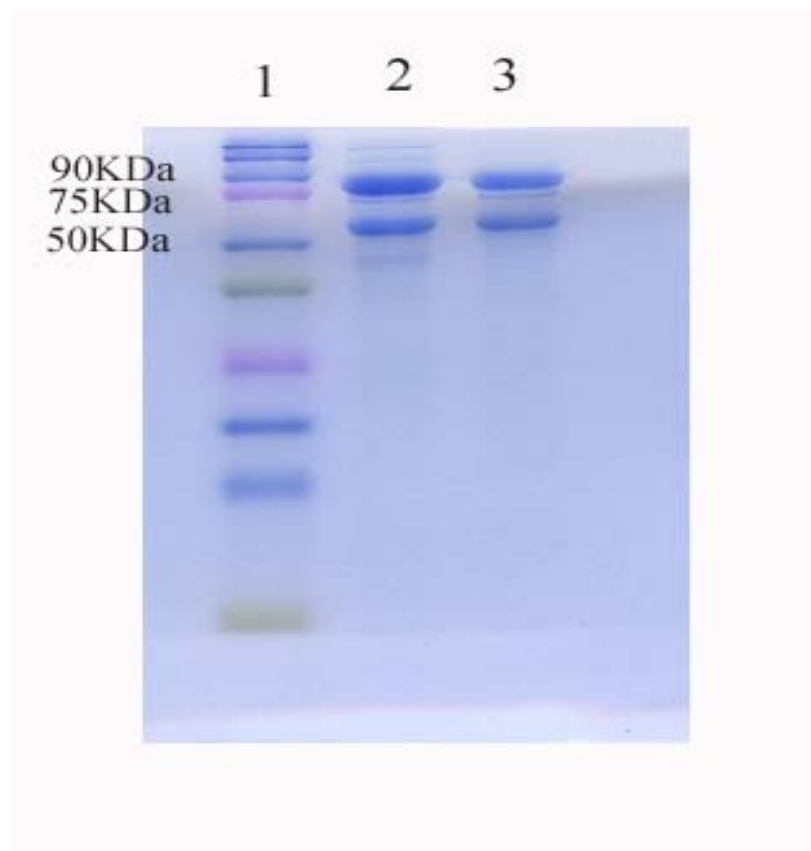


Figure 4. Coomassie stained SDS-PAGE gel analysis of recombinant Arg355Met XDH_{ABC}. Lane 1: Molecular Weight Standards Lane 2: Wild-type XDH Lane 3: Arg355Met XDH

2.3.2 Characterization of recombinant Arg355Met from *P. aeruginosa* PAO1-LAC

2.3.2.1 Chemical properties and Spectral properties of recombinant Arg355Met

XDH

The UV-Vis spectrum of the Arg355Met mutant enzyme (Fig 5) is very similar in shape to the spectrum of wild-type in both the oxidized and reduced states. The shape of the oxidized recombinant Arg355Met mutant XDH spectrum, similar to that of the wild-type enzyme ^[15], features the characteristic absorption bands of the flavin (450 and 370 nm) and of the 2 [2Fe-2S] clusters (467 and 420 nm). A contribution to the visible absorption spectrum is also expected from the absorption of Moco. Differences between the levels of reduction are observed in the absorption at 450 nm when 1mM xanthine and dithionite crystals are added. Bleaching of the visible absorption spectrum is due to the reduction of the iron-sulfur and FAD cofactors. The similarity between the Arg355Met XDH and the WT XDH in both oxidized and reduced absorption spectrum suggests the presence of identical sets of stoichiometrics of the cofactors ([2Fe-2S] centers and FAD). The stoichiometry of the iron-sulfur centers is further confirmed by the metal analysis result which shows a ratio of 4.05 Fe/Flavin in the Arg355Met mutant enzyme. The metal analysis result also shows the content of molybdenum in the mutant enzyme is 0.49Mo/Flavin, however only 11% of Mo is in the sulfurated functional form, which is obtained from the determination of functionalized Mo content experiments with Sorbo

reagent ^[79]. The low functionality of the mutant enzyme shows that the mutation of Arg355 to Met causes the Mo sulfuration to be less efficient.

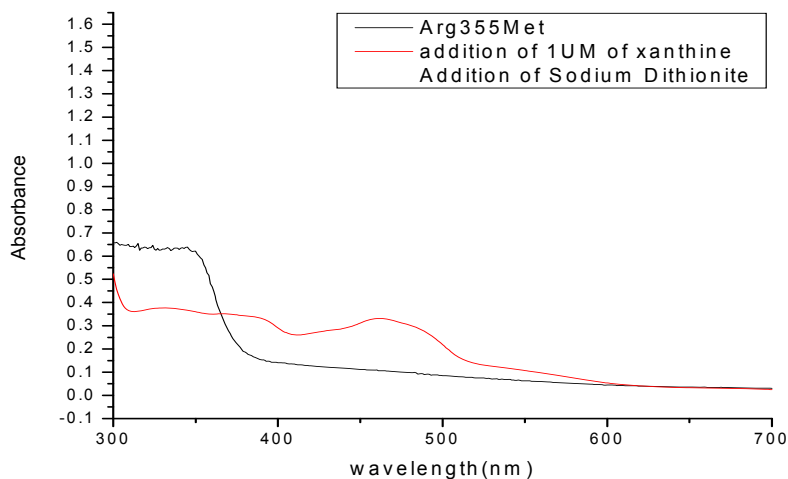


Figure 5 UV-Vis of recombinant Arg355Met XDH_{ABC} expressed in *P. aeruginosa*: oxidized (red line) and anaerobically reduced with dithionite (black line).

Previous studies have shown that a good test for the integrity of the two oxidized Fe₂S₂ clusters in XO/XDH is to measure the Circular Dichroism (CD) spectrum in the visible spectral range, and these clusters dominate the visible dichroism behavior of XO/XDH. The Arg355Met mutant enzyme shows an identical CD spectrum with that of the wild-type CD spectrum Figure 6. The overall shape of the spectra is very similar to that of *C. acidovorans* wild-type enzyme with two characteristic intense positive dichroic bands with maximum at around 470 nm and 430 nm as typical of the oxidized [2Fe-2S], and two negative bands with maxima at around 375 nm and 565 nm ^[15]. Moreover, the molar ellipticity $[\theta]$ equals to $1.74 \times 10^5 \text{ deg}\cdot\text{cm}^2\cdot\text{dmol}^{-1}$ for recombinant Arg355Met,

which is very close to $1.75 \times 10^5 \text{ deg}\cdot\text{cm}^2\cdot\text{dmol}^{-1}$ for the WT XDH. The result indicates that the mutant enzyme has two [2Fe-2S] identical to the WT XDH ^[15].

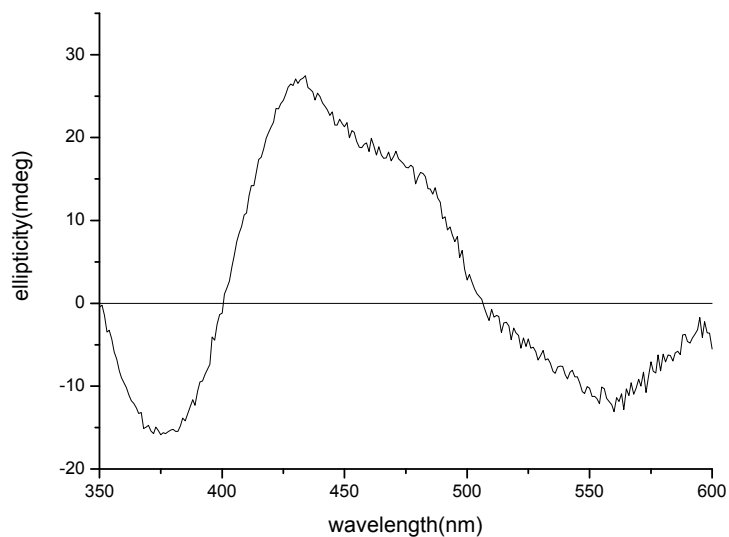


Figure 6. Circular Dichroism (CD) of oxidized recombinant Arg355Met XDH_{ABC} (15.8 μM) expressed in *P. aeruginosa*

Table 3 Comparison of the properties of Wild-type and Arg355Met *C. acidovorans* XDH, steady state kinetic parameters were measured at PH 7.8

Properties	Wild-type XDH _{ABC}	Arg355Met XDH _{ABC}
Mo=S	0.86 ^[15]	0.11
Specific activity/Mo=S for xanthine(U/mg functionalized enzyme)	93±6 ^[15]	0.35
Specific activity for phenanthridine/Mo=S (U/mg functionalized enzyme)	N.D ^d	0.34
Specific activity for benzaldehyde/Mo=S (U/mg functionalized enzyme)	4.77	16.9
Specific activity for N-methylnicotinamide	N.D. ^d	N.D ^d
$k_{cat}(s^{-1})$ for xanthine /Mo=S	255±8 ^[15]	0.83±0.018
$k_{cat}(s^{-1})$ for phenanthridine /Mo=S ^a	N.D ^d	0.72±0.013
$k_{cat}(s^{-1})$ for benzaldehyde /Mo=S ^b	65.25±0.10	186.27±5.45
$k_{cat}(s^{-1})$ for purine/Mo=S	13.07±0.15	14.86±0.35
$k_{cat}(s^{-1})$ for hypoxanthine /Mo=S	226.9±1.69	8.27±0.37
K_M xanthine (μM)	120±5 ^[15]	100±8.7
K_M phenanthridine(μM)	N.D. ^d	61.06±3.17
K_M benzldehyde (μM)	14944.1±12.27	4054.5±294.7
K_M NAD ⁺ (μM)	81±14	107.8±3.7 ^c
K_M purine (μM)	271.0±24.1	252.1±14.2
K_M for hypoxathine (μM)	106.1±3.0	5102.96±322.74

a The kinetics parameters of wild-type for phenantridine was determined by the wild-type with the Mo=S as 66%

b The kinetics parameters of wild-type for benzaldehyde was determined by the wild-type with the Mo=S as 66%

c The K_m NAD⁺ was obtained by Lineweaver-Burk plot

d. N.D Not detectable

2.3.2.2 Kinetic parameters of recombinant Arg355Met at pH 7.8

Table 3 summarizes kinetic parameters measured at pH 7.8 for Arg355Met *C. acidovorans* XDH compared with that for wild-type XDH [15]. The specific activity and turnover numbers are recalculated per amount of functional enzyme (Mo=S) because of the different content of Mo sulfuration exhibited by the WT enzyme and the mutant. The comparison of the kinetic parameters reflects the large catalytic difference between WT and the mutant. For Arg355Met, $k_{cat}/\text{Mo=S}$ of xanthine is only 0.83 s^{-1} (0.33% of WT), which indicates a crucial role for Arg355 in the hydroxylation of xanthine. Observed K_M values do not change much for the Arg355Met with xanthine as the substrate, and K_M value for xanthine of Arg355Met at pH 7.8 is only slightly less than that for the wild-type (83% of the K_M for wild-type XDH). On the other hand, K_M for NAD^+ is found to be about 1.3 fold higher than the value exhibited by the wild-type enzyme.

For hypoxanthine, another substrate of XDH, the Arg355Met shows only 3.6% activity for turnover numbers as the WT, and the K_m for the mutant is about 48-fold of that for the wild-type. This result further confirms the important role that Arg355 plays in XDH catalysis.

The K_m value of the Arg355Met XDH for purine is at the same value within the error as that of wild-type enzyme, as do the turnover numbers of the mutant ($14.86 \pm 0.35 \text{ s}^{-1}$) and for that of wild-type ($13.07 \pm 0.15 \text{ s}^{-1}$). The data indicate that replacing Arg355 does not take much effect on the oxidation of purine.

The Arg355Met mutant shows activity ($k_{cat}(s^{-1})/Mo=S$ for phenanthridine as $0.72\pm 0.013 s^{-1}$) with phenanthridine, a typical substrate for AO, whereas WT XDH exhibits no detectable activity with this substrate. The increase in the activity with the substrate of AO provides evidence that Met in this position is more important for the oxidation of phenanthridine than Arg.

Both wild-type and Arg355Met XDH demonstrate activity for benzaldehyde oxidation, a common substrate of both XDH and AO. Arg355Met XDH shows a larger specific activity than the wild-type XDH, and it is consistent with the fact that K_m of Arg355Met XDH ($4054.5\pm 294.7 \mu M$) is 3.7 times smaller than the K_m of the wild-type enzyme ($14944.1\pm 12.3 \mu M$).

Neither Arg355Met nor WT XDH shows any detectable activity with N-methylnicotinamide, a well-known mammalian AO substrate.

Determination of the product obtained by oxidation of phenanthridine through Arg355Met *C. acidovorans* XDH

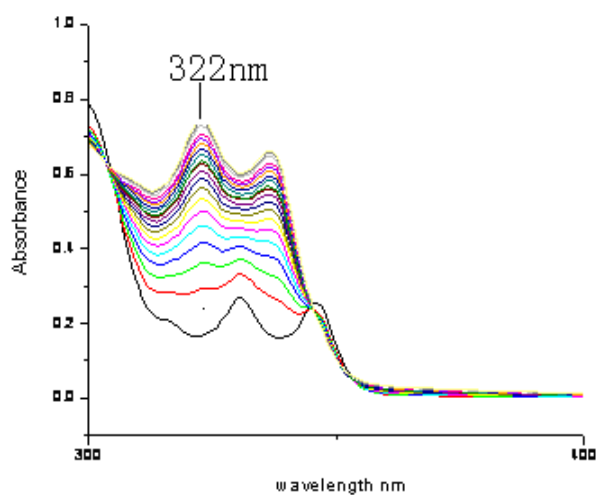
To confirm the oxidation of phenanthridine by Arg355Met XDH is identical with that expected for AO oxidation of this compound, the properties of the oxidation of phenanthridine were determined.

Figure 7(A) shows the UV-Vis spectroscopic changes after adding the mutant enzyme to $60 \mu M$ of phenanthridine solution, using O_2 as electron acceptor, and Figure 7(B) shows the UV-Vis spectrum of 6-phenanthridone. With increases in reaction

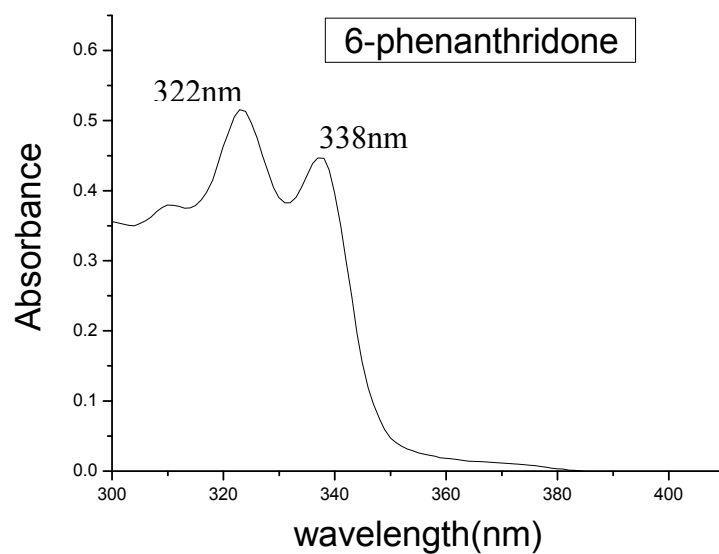
time, the peak at 322 nm increases which indicates the appearance of 6-phenanthridone, which has been shown to be product of phenanthridine oxidization by aldehyde oxidase [80]. The isosbestic points at 310 nm and 345 nm demonstrate only a simple conversion of substrate to product process.

To further confirm the product of oxidation of phenanthridine by Arg355Met XDH, thin layer chromatography (TLC) is performed by eluting the product, pure 6-phenanthridone and phenanthridine in silica gel 60 plates using volume ratio of ethyl acetate to hexane as 1:3 (v/v).

The result of TLC is shown in Figure 8. Lane 2 on the TLC plate shows the presence of 6-phenanthridone in the final product extracted from the reaction solution. This further proves the product of phenanthridine oxidation by Arg355Met XDH is 6-phenanthridone, which is the same product as oxidized by AO.



(A)



(B)

Figure 7 (A) Changes in the UV-Vis spectra monitored at the 20 mins interval after adding 0.006U of Arg355Met to the TE buffer solution containing 60 μ M phenanthridine. (B) UV-Vis spectrum of 6-phenanthridone

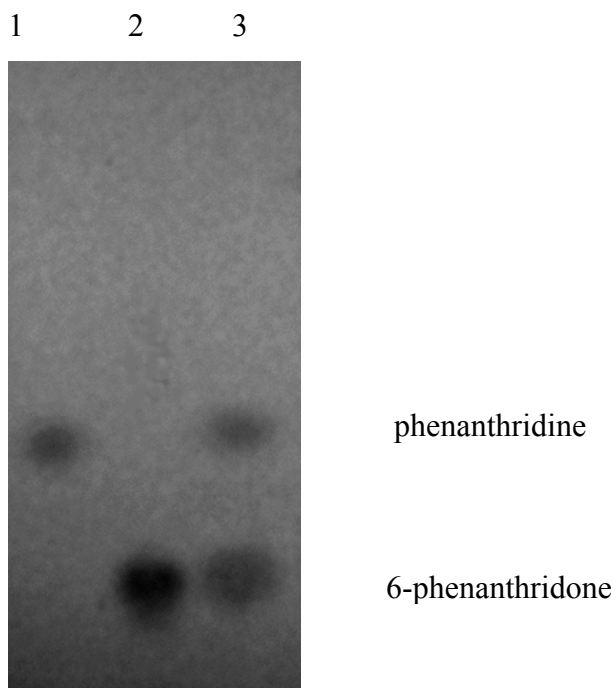
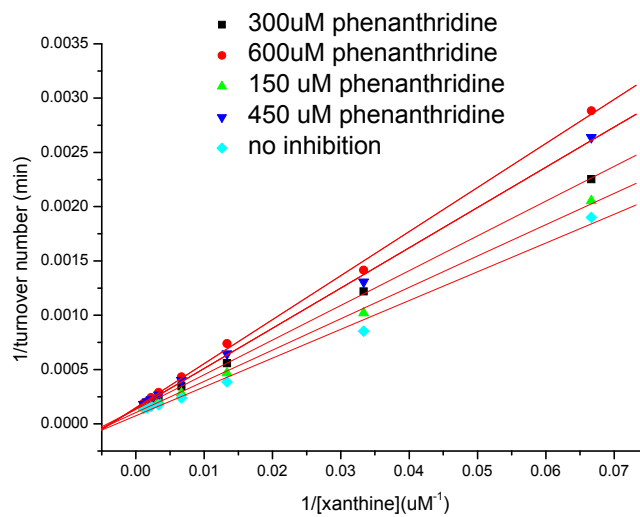


Figure 8 TLC result on silica gel 60 plates using EtOAc : Hexane = 25 : 75 as solvent. Lane 1: phenanthridine; Lane 2: 6-phenanthridone, Lane 3: Mixture of

phenanthridine and 6-phenanthridone obtained from oxidation of phenanthridine catalyzed by the Arg355Met XDH

Determination of Inhibition constant of phenanthridine for WT XDH

Figure 9 demonstrates the competitive inhibitory activity of phenanthridine from 0 μM to 600 μM on the oxidation of xanthine by WT XDH. The kinetic analysis of the reaction revealed that phenanthridine exerts its inhibitory effect on wild-type XDH in a competitive type of inhibition to xanthine, and the K_i value inhibitory constant is 689.6 ± 37.5 μM , which is 11 fold higher than the K_m value of phenanthridine for the Arg355Met XDH.



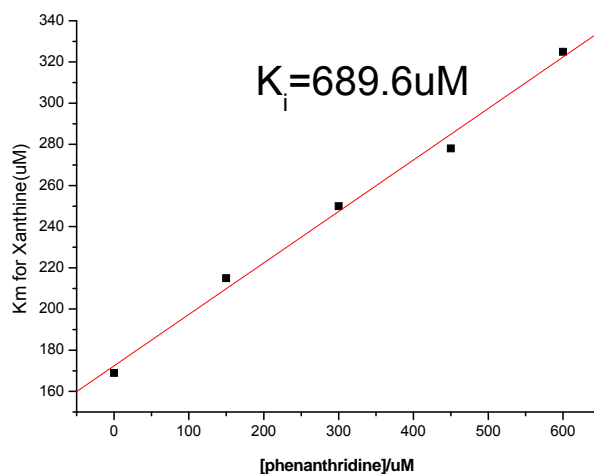
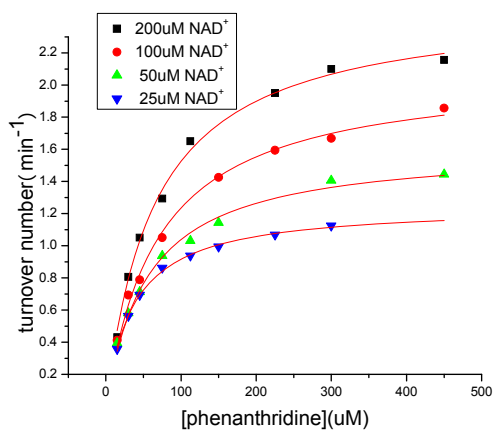
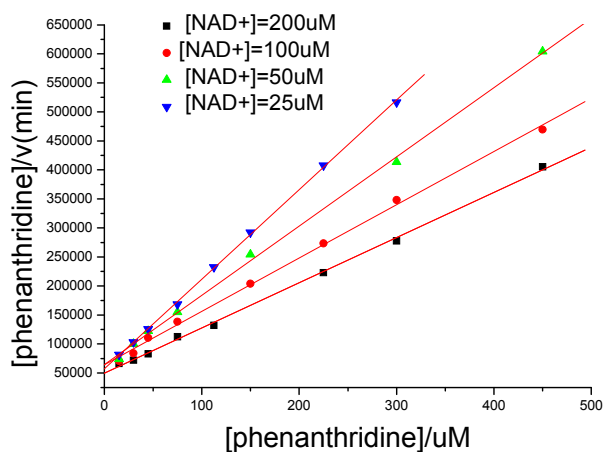


Figure 9 (A) Typical Lineweaver-Burk plots for Inhibitory activity of phenanthridine on the oxidation of xanthine by *C. acidovorans* XDH (B) K_m change with the inhibitor concentration.

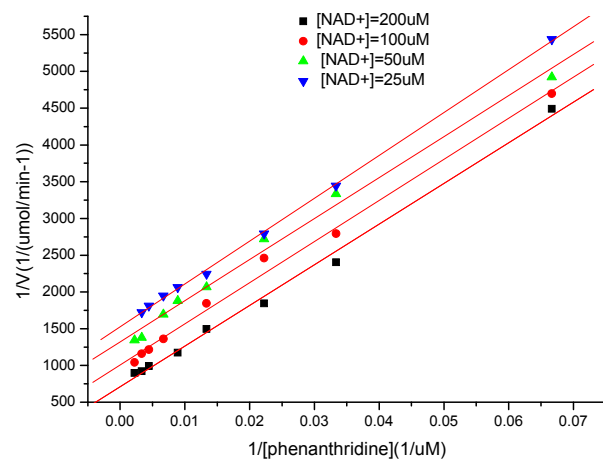
2.3.5 Kinetics analysis for reactions of NADH and 6-phenanthridone formation



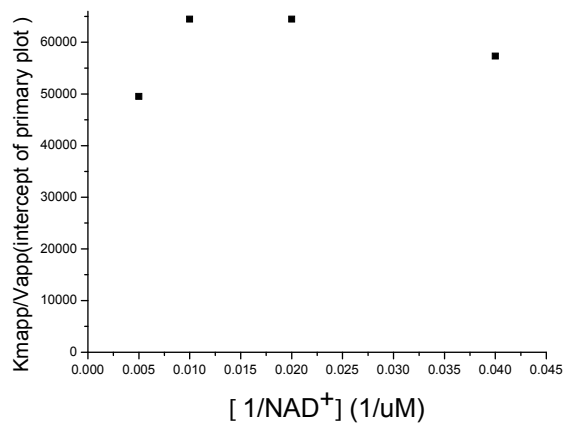
(A)



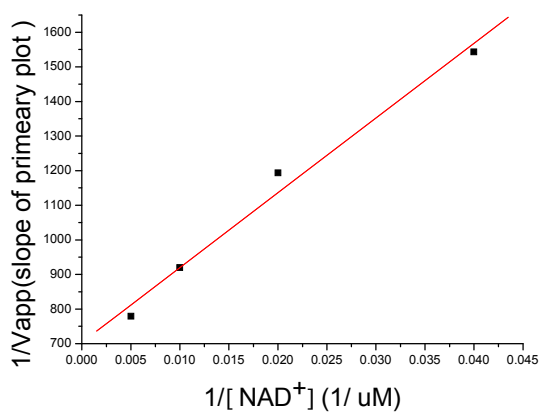
(B)



(C)



(D)



(E)

Figure 10. Kinetics analysis for reactions of NADH and phenanthridone formation
(A) kinetics of the reaction between phenanthridine and NAD⁺ catalyzed by Arg355 Met XDH. K_{mapp} phenanthridine and V_{appmax} values at different NAD⁺

concentrations can be determined by fitting the data to Michaelis-Menten equation. (B) Primary plots (Hanes plots) of the kinetics of the reaction between phenanthridine and NAD^+ (C) Primary plots (Lineweaver-Burk plots) of the kinetics of the reaction between phenanthridine and NAD^+ (D) & (E) Secondary plots of the kinetics of the reactions between phenanthridine and NAD^+ catalyzed by Arg355Met XDH. K_m phenanthridine was calculated using its intercept ($K_m \text{ phenanthridine}/V_{\text{max}}$). $K_m \text{ NAD}^+$ was calculated using its intercept ($1/V_{\text{max}}$) and slope ($K_m \text{ NAD}^+/V_{\text{max}}$).

The kinetics of NADH and 6-phenanthridone formation is investigated as a function of phenanthridine and NAD^+ concentrations. Results for the reactions of phenanthridine with NAD^+ are shown in Figure 10(A). Primary plots (Hane plots) are shown in Figure 10(B), and primary plots (Lineweaver-Burk plots) are shown in Figure 10 C. The slopes of ($1/V_{\text{app}}$) and intercepts ($K_{\text{app}}/V_{\text{app}}$) of the Hanes plots are derived and used in the secondary plots are shown in Figure 10 (D) and (E). (D) is used to calculate the K_m phenanthridine values using its intercept ($K_m \text{ phenantrhidine}/V_{\text{app}}$), and (E) is used to calculate the $K_m \text{ NAD}^+$ values using its intercept($1/V_{\text{app}}$). The $K_m \text{ NAD}^+$ and K_m phenanthridine from the secondary plots are $30.8 \pm 3.2 \mu\text{M}$ and $78.2 \pm 4.7 \mu\text{M}$, which is comparable with the $107.8 \pm 3.7 \mu\text{M}$ and $61.1 \pm 3.2 \mu\text{M}$ for the two substrates from Michaelis-Menten plots respectively.

Discussion

The pUCP-Nde/*P. aeruginosa* expression system allows expression of Arg355Met *C. acidovorans* XDH in high yield, as previously found for the WT enzyme [15]. Arg355Met recombinant XDH exhibits UV-Vis and CD spectral properties very

similar to those of wild-type enzyme, which indicates the intactness of the flavin cofactor and the two [2Fe-2S] in the Arg355Met XDH.

For the purification steps, the enzyme yields for two substrates are similar after the DE-52 column, but quite different in the crude extract (Table 2). This may be because there is another enzyme activity in the crude cell extract of *P. aeruginosa* that catalyzes phenanthridine oxidation in addition to that of the mutant XDH from *P. aeruginosa*. The activity of crude extract of wild-type enzyme was measured for phenanthridine to confirm this assumption. The crude extract of the wild-type enzyme exhibits a specific activity for phenanthridine oxidation as 0.001 U/mg which is not detected in the purified enzyme, and in this way the unknown enzyme accounts for 0.46 U/L activity for phenanthridine in the crude extract of mutant. However, there is still another 1.6 U/L activity for phenanthridine unaccountable.

Kinetic characterization of Arg355Met *C. acidovorans* XDH at pH 7.8 reveals the catalytic function change for the mutant with respect to the WT enzyme upon the one single amino acid change. k_{cat} values recalculated for the amount of functional molybdenum (Mo=S) with xanthine and hypoxanthine reflect a difference of about 1 and 2 orders of magnitude separately between Arg355Met XDH and WT XDH. The difference in catalytic activity translates in a $\Delta(\Delta G)$ for the reaction that we determined to be ~ 2.0 Kcal/mol and ~ 3.4 Kcal/mol for Arg355Met with respect to the WT enzyme for hypoxanthine and xanthine. This considerable gap in ΔG documents the crucial role of

Arg in the catalytic process of oxidation of xanthine, which is consistent with the result that changing of the corresponding Arg residue to Gln or Gly in *Aspergillus nidulans* XOR^[72]. This result further confirms the important role of Arg355 in *C. acidovorans* in positioning the xanthine substrate.

The k_{cat} value for Arg355Met XDH with hypoxanthine as the substrate decreased 27 fold, and the K_m value increased 48 fold, compared with the values for the wild-type XDH. These results are consistent with the reported data from Nishino's group^[81] on the R881M human XOR which showed the k_{cat} with hypoxanthine was 90 times lower and the K_m value was 12 times larger as compared with WT enzyme. The catalytic efficiency k_{cat}/K_m was decreased 1330 fold with the Arg355Met *C. acidovorans* XDH, which is very close to 1064 times lower as reported for Arg881Met Human XOR. The *C. acidovorans* XDH does show similar characteristics for the mammalian enzymes. However, the kinetics parameters with xanthine for Arg881Met human XOR were not known due to the low activity of the mutant enzyme. The high yields of pUCP-Nde/*P. aeruginosa* expression system provided us the possibilities of complete kinetics studies on the mutant.

Purine is also a typical substrate for wild-type XDH, but the turnover number and the K_m value for Arg355Met XDH are quite similar with those determined for WT XDH, which suggests changing Arg355 to Met does not influence the kinetic properties of purine oxidation. This result, compared with the 99.7% decrease in turnover numbers for

xanthine and 96% decrease with hypoxanthine, shows the Arg355 is essential for positioning xanthine and hypoxanthine in the active site, but not purine. This positioning is suggested to occur by an Arg interaction with the O in substrates, probably by H-bond interactions which plays an important role in substrate orientation in the catalytic mechanism.

Arg355Met XDH shows activity with phenanthridine, which is a typical substrate for AO, as the drastic difference with WT XDH which does not show detectable activity with it. Met at this position plays a more important way for oxidation of phenanthridine than Arg. The K_m of phenanthridine of the mutant is $61.1 \pm 3.2 \mu\text{M}$; relative to reported $K_m = 4.1 \pm 1.5 \mu\text{M}$ [82] of phenanthridine for AO, the mutant has less capability of catalyzing phenanthridine. Both wild-type and Arg355Met XDH demonstrate activity with benzaldehyde oxidation, a common substrate of both xanthine dehydrogenase and aldehyde oxidase. Arg355Met XDH shows a larger specific activity for benzaldehyde than the wild-type XDH, and it is consistent with the K_m of Arg355Met XDH ($4.1 \pm 0.3 \text{ mM}$) is 3.7 times smaller than the K_m of the wild-type enzyme ($14.9 \pm 0.1 \text{ mM}$). On the other hand, the K_m of benzaldehyde for guinea pig liver aldehyde oxidase is reported as $13.4 \pm 3.1 \mu\text{M}$ [82] which is much smaller than the mutant and wild-type XDH. The catalytic efficiency which is represented by k_{cat}/K_m for Arg355Met mutant enzyme is $0.046 \mu\text{M}^{-1} \cdot \text{s}^{-1}$, which is much higher than the value for the wild-type enzyme $0.004 \mu\text{M}^{-1} \cdot \text{s}^{-1}$, but still much smaller than k_{cat}/K_m value for aldehyde oxidase reported as $101.4 \mu\text{M}^{-1} \cdot \text{s}^{-1}$.

¹.s¹ [83]. The decrease of K_m for benzaldehyde and increase in the value of k_{cat}/K_m after mutation further confirms the partial conversion of XDH to one with ADH activity by this single point mutation Arg355Met. The kinetics parameters for Arg881Met human XOR with benzaldehyde show similar results as data from our mutant, with the K_m value decreasing by 2.2 fold, k_{cat} value increasing 2.7 fold, and the k_{cat}/K_m increasing 5.7 fold on the mutation [81].

The increase in the AO activity for phenanthridine and benzaldehyde shows the single amino acid change can realize the conversion of the catalytic function of XDH to that of an ADH; on the other hand, the increase in the AO activity for phenanthridine and benzaldehyde after mutation provides evidence that aldehyde oxidation favors a Met group more than an Arg group. The function of Met in aldehyde oxidation in AO is still under investigation. The Arg355Met shows a less substrate affinity for phenanthridine and less catalytic activity for benzaldehyde than Guinea pig liver AO, supporting the fact that neither of Arg355MetXDH and wild-type XDH has detectable activity with the N-methylnicotinamide which is a specific substrate of AO. There are other residues in the active site that are also play important roles in the oxidation mechanism of aldehyde oxidase with phenanthridine and N-methylnicotinamide, which are absent in XDH.

Conclusion and future work

With the aid of high-level expression system pUCP-Nde/P. *aeruginosa*, Arg355Met active site mutant of *C. acidovorans* XDH was expressed and characterized.

The Arg355Met XDH maintains the structural integrity of the wild-type XDH by showing similar UV-Vis and CD optical properties as the wild-type enzyme, indicating the similar structures of cofactor sites in the mutant enzyme. Through a comparison of the kinetic parameters of the mutant with those of the wild-type enzyme, the mutant is shown to maintain the function of the wild-type by showing 0.3% and 3.6% of activity for xanthine and hypoxanthine hydroxylation, and the lower activity relative to the wild-type enzyme indicates an important role of Arg355 in the oxidation of xanthine. On the other hand, the mutant Arg355Met shows activity with phenanthridine, a substrate of aldehyde oxidase, whereas the wild-type enzyme exhibits no activity. Furthermore, the Arg355Met XDH demonstrates 11-fold increase in catalytic efficiency for benzaldehyde oxidation than does the wild-type XDH, closer to the catalytic properties of aldehyde oxidase. These results demonstrate the possibility of the conversion of an enzyme with altered substrate specificities closer to that of an aldehyde dehydrogenase through one single point mutation. This accomplishment also confirms the validity of the computational analysis result by the Diverscan program. The finding of the same product of phenanthridine oxidation by Arg355Met XDH as with aldehyde oxidase suggests similar mechanisms and catalytic pathways for XDH and AO catalysis.

Chapter III

Investigation of the Catalytic Mechanism of *C. acidovorans* Xanthine Dehydrogenase: Characterization and Kinetic Studies on the Glu758Gln Active-site Mutant

3.1 Introduction

Products and byproducts generated during XORs catalytic cycle are not only of physiological importance but also of great medical interest. Due to the medical relevance of the biological reaction catalyzed by XORs, the different aspects of the catalytic mechanism of these enzymes have been intensively investigated through the years^[31, 34-36, 40, 42, 84]. Several mechanisms for the reductive half reaction of Xanthine Oxidoreductases have been proposed^[40, 42]. In the past, the absence of details about the structure of the active site and a lack of a high-level expression system to permit site-directed mutagenesis required that insights into the catalytic mechanism relied on experimental data coming from EPR spectroscopy, EXAFS^[40, 84], Raman spectroscopy^[44], and from analysis of the kinetic properties of the bovine enzyme^[32]. EPR spectroscopic studies have demonstrated the formation of a Mo(V) (very-rapid) intermediate with a Mo-O-C bond. Single couplings of the very rapid Mo(V) signal to ¹⁷O^[84] and to ¹³C^[40] were detected in active bovine xanthine oxidase. Moreover, isotope effect and pH dependence studies on bovine milk XO^[32] revealed small substrate isotope effect (1.7), a larger solvent isotope effect (3.5), and a bell-shaped pH dependence of the activity that suggested two pK_a values (pK_{a1} = 6.6 and pK_{a2} = 7.4) of ions of the groups

involved in the catalytic mechanism. The pK_{a2} at 7.4 was assigned to the substrate, whereas the 6.6 pK_{a1} was assigned to either the Mo-OH or to the Mo-SH groups.

In the substrate binding sites of XDH, there are several highly conserved amino acid residues: Phe914 (in the *B. Taurus* XOR numbering), Phe1009, Glu802, Glu1261 and Arg880 (Figure 1). It has been suggested that substrate intercalates between the phenylalanine residues in binding to the active site based on the crystal structures of the *R. capsulatus* XDH with the inhibitor alloxanthine ^[71] and the structure of the bovine enzyme with FYX-051 ^[85]. The two Glu residues are on opposite sides of the substrate binding cleft defined by the phenylalanines. Glu802 and Glu1261 are within the hydrogen-bonding distance to the substrate and the molybdenum center respectively. Among these four residues, Glu1261 is universally conserved, however, Glu802 and Arg880 are not conserved in the aldehyde oxidases which is similar to XDH in the molybdenum-containing hydroxylase family ^[1].

The mechanism proposed by R. Hille in 1999 for milk XO ^[42] suggests the presence of basic residues at the enzyme active site involved in an acid-base activation pathway for substrate hydroxylation. Recent mutagenesis studies on *R. capsulatus* XDH ^[86] have shown that mutation of Glu232 (corresponding to Glu802 in bovine XO, ~5 Å from the Mo atom) to Ala results in a decrease in enzyme activity of ~20-fold. On the other hand, mutation of Glu730 (corresponding to Glu1261 in bovine XO, ~3 Å from the Mo atom) to Ala, Gln, Arg or Asp results in a completely inactive enzyme. These data

demonstrate the importance of these two Glu residues for the enzyme activity, and led to the hypothesis that the catalytic base proposed in Hille's mechanism could be assigned to Glu730 in *R. capsulatus* XDH or to Glu1261 in bovine XO [85, 86]. However, the acid/base role of this Glu residue has not clearly been proven and the details of the catalytic mechanism of xanthine oxidoreductases are still not completely understood.

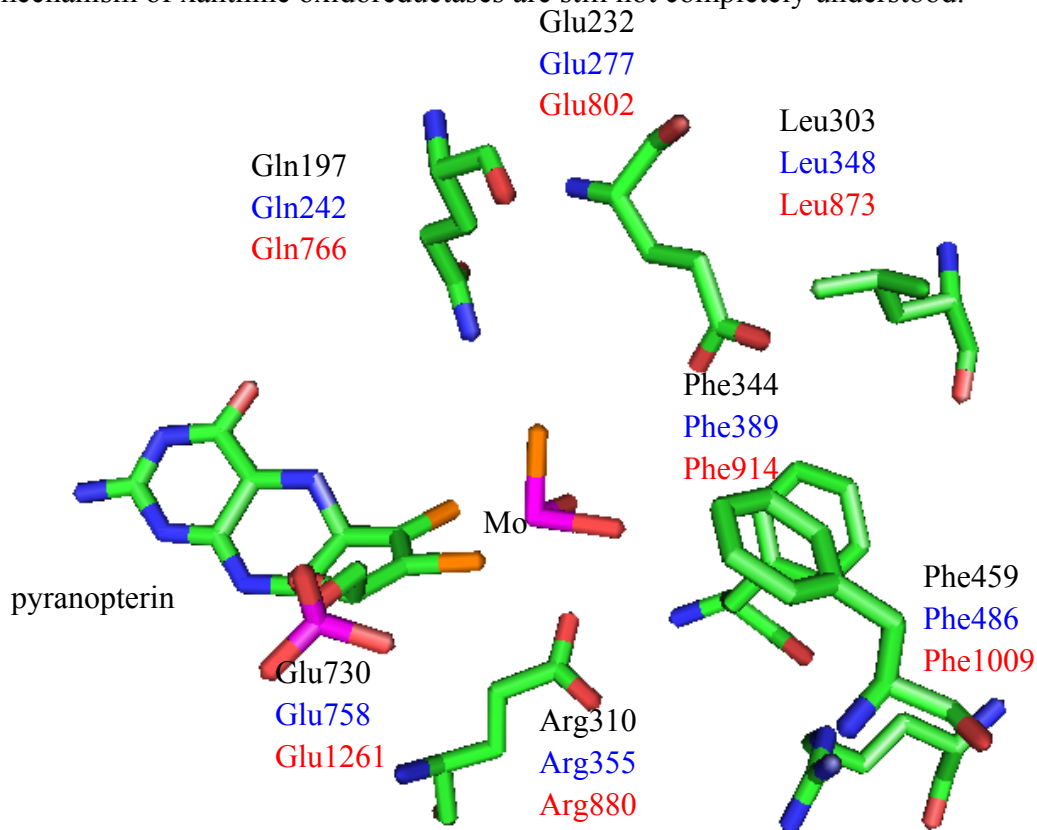


Figure 1. Active site of *R. capsulatus* XDH (Pymol view)
In parentheses are reported the equivalent residues of *C. acidovorans* XDH (blue) and *B. Taurus* XO (red) on the basis of sequence alignment.

Recent cloning and sequencing of the gene for *C. acidovorans* XDH [19] show that active site residues are conserved in this prokaryotic XDH as in *B. Taurus* XO and in *R. capsulatus* XDH (Figure 1). *C. acidovorans* Glu758 is likely to be structurally equivalent

to *R. capsulatus* Glu730, and *B. Taurus* Glu1261. With the aid of the high-level expression system pUCP-Nde/*P. aeruginosa* recently developed in our laboratory for *C. acidovorans* XDH, *xdhABC* Glu277Gln and Glu758Gln mutants were already expressed by Dr. Manuela Trani. This chapter describes the expression of Glu758Gln and the compares the characterization of WT and Glu758Gln *C. acidovorans* XDH. The separation of the endogenous XDH in *P. aeruginosa* and expressed Glu758Gln mutant XDH is also included in this work.

3.2 Materials and Methods

3.2.1 Materials

P. aeruginosa PAO1-LAC was used as an expression host and was maintained on Luria-Bertani plates supplemented with 15 g/mL tetracycline.^[76] The *P. aeruginosa* strains, pMT801 for Glu758Gln was a gift from Dr. Trani. Ni-NTA resin was from Qiagen. All other reagents were purchased from either Sigma-Aldrich Co. (St. Louis, MO), Fisher Scientific Co. (Pittsburgh, PA), or Denville Scientific (New Jersey).

3.2.2 Expression and purification of recombinant Glu758Gln XDH

P. aeruginosa strains, pMT801 for Glu758Gln was grown as previously reported.^[15] Cells harvesting, breakage and enzyme purification schemes were also the same as previously described for the wild-type enzyme^[15], except that a linear imidazole gradient 5 mM-150 mM was used in elution from the Ni-NTA column for Glu758Gln to separate the endogenous XDH in *P. aeruginosa* from the expressed mutant.

3.2.3 Characterization of recombinant Glu758Gln XDH

UV-Vis absorption spectra were measured either on Lambda 2 spectrometer (Perkin-Elmer, Boston, MA) or a Cary 50 UV-VIS spectrophotometer (Varian Inc., Walnut Creek, CA) at 25 °C. Circular Dichroism (CD) spectra were recorded in an average of six-eight scans on CD spectrometer AVIV model 62SD at 25 °C using anaerobic quartz cuvettes.

XDH activity was measured by following the appearance of uric acid at 295nm ($\epsilon_{295}=9600 \text{ M}^{-1} \text{ cm}^{-1}$) at 25 °C in TE buffer (100 mM Tris-HCl, 1 mM EDTA, pH 7.8) with the addition of freshly prepared 15 mM xanthine and 50 mM NAD^+ to a final concentration of 0.6 mM xanthine and 2 mM NAD^+ , respectively. One unit of enzyme activity is defined as the amount of enzyme required to produce 1 μ mol of uric acid in one minute at 25 °C. Kinetic properties at pH 7.8 were measured by monitoring NADH formation on Luminescence Spectrometer (AMINCO. BOWMAN series 2) at 25 °C in TE buffer (100 mM Tris, 1 mM EDTA, pH 7.8) using xanthine concentrations ranging between 15 and 900 M. The excitation wavelength and the emission wavelength for luminescence spectrometer were set up at 340nm and 460nm separately, with the bandpass at 4 nm. The detector high voltage was set up at 790 V. Steady state kinetic parameters were calculated for xanthine and NAD^+ by non linear fitting to the Michaelis Menten equation using Origin 7.0.

The Biuret assay ^[77] was used to estimate protein concentration in cell extracts and after the first purification step. For later steps concentrations of purified enzyme were determined spectrophotometrically at 450 nm ($\epsilon_{450} = 37,000 \text{ M}^{-1} \text{ cm}^{-1}$).

SDS-PAGE gels 7.5% were prepared according to Laemmli ^[78]. Western blot detection was performed using rabbit polyclonal antisera raised against purified *C. acidovorans* XDH ^[10] in a 1:2000 dilution and goat anti-rabbit IgG Alkaline Phosphatase conjugate (Sigma Co.) in 1:3000 dilution. Alkaline phosphatase substrate Sigma Fast BCIP/NBT tablets were used for visualization. For xanthine-NBT activity staining, protein samples were separated on 7.5% native gel electrophoresis following the same procedure except that no SDS in sample buffer or running buffer, and no heat treatment to the sample. XDH active bands were stained using 0.6 mM xanthine, 50 mM KPi, pH 7.8, 0.1 mM EDTA, 0.4 mM nitrobluetetrazolium (Sigma) and 0.2 mM phenazinemethosulfate (sigma) in the dark for at least 20 mins. ^[29]

Metal analyses on the purified enzymes were performed with a Jarrell-Ash 965 ICP Plasma Emission Spectrometer at the Chemical Analysis Facility at University of Georgia in Athens, GA.

Functionality (level of sulfurated Moco) of wild-type and mutant enzymes were measured on solutions containing 30 nmoles by analytical determination of the amount of SCN^- released by the enzymes upon treatment with CN^- according to the method described by Sorbo ^[79].

3.3 Results

3.3.1 Expression and purification of recombinant Glu758Gln in *P. aeruginosa*

PAO1-LAC

Table 1. Purification steps for endogenous XDH in *P. aeruginosa* ^a

	Total protein(mg)	Total activity(U)	Specific activity(U/mg)	Yield(%)
Crude extract	590.4	0.6723	0.00114	100
Ni-NTA column	4.7	0.1323	0.0028	20

a Recalculated for 1 L of culture

Glu758Gln were expressed and purified from *P. aeruginosa* PAO1-LAC following the similar procedure used to express and purify the WT recombinant enzyme. As in the WT enzyme, the mutant was His-tagged at the N-terminus of the β subunit to allow purification with metal affinity chromatography. The pUCP-Nde/*P. aeruginosa* system is very efficient for the expression of mutant forms of *C. acidovorans* XDH. Unlike Glu277Gln, which has higher activity ^[87], Glu758Gln was purified from Ni-NTA column, with 5 mM-150 mM imidazole gradient to separate any endogenous XDH from *P. aeruginosa*. Table 1 summarizes the purification steps and enzyme yields for the endogenous XDH in *P. aeruginosa*. Endogenous XDH in *P. aeruginosa* does bind to the Ni-NTA column although it is not His-tagged, and when the activity of the endogenous XDH in *P.aeruginosa* is comparable with that of the expressed *C.acidovorans* mutant XDH as Glu758Gln mutant, the endogenous one has to be removed since its activity can influence the results observed for the mutant enzyme.

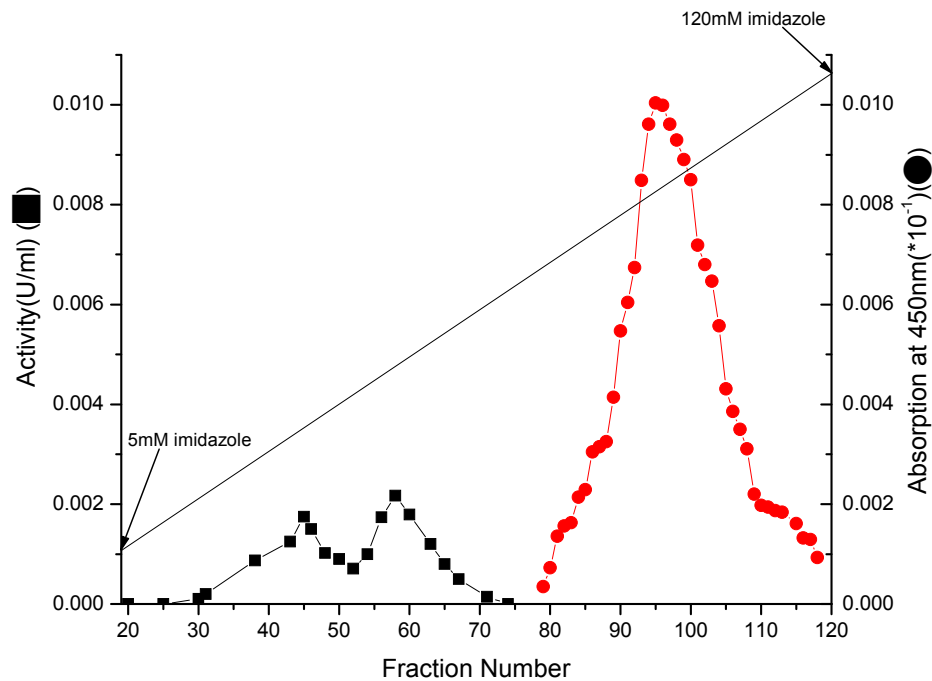


Figure 2. Ni-NTA column chromatography of Glu758Gln *C.a* XDH. Eluants were collected in 6.5ml fractions. ■, protein determined by measuring the activity level, ●, protein determined by measuring the absorbance at 450nm

Figure 2 shows the presence of peaks of *P. aeruginosa* XDH and expressed Glu758Gln XDH after eluting the Ni-NTA column with the imidazole gradient. The first two peaks with the imidazole concentration at 35mM and 50mM are the endogenous XDH in *P. aeruginosa*, which is consistent with the imidazole concentration when eluting Ni-NTA with imidazole gradient for endogenous XDH in *P. aeruginosa* only. Figure 3 shows the native gels of the two peaks of endogenous XDH in *P. aeruginosa*. The two peaks migrate the same distance on the gel but with differing imidazole concentrations, this difference in elution behavior on the Ni-NTA column might be because of two different modes of binding. The peak with the imidazole concentration

around 90 mM, which is the aligned according to the absorbance at 450 nm, is assigned to the peak of the expressed Glu758Gln XDH. After the endogenous XDH in *P. aeruginosa* was removed, the expressed Glu758Gln mutant XDH was separated.

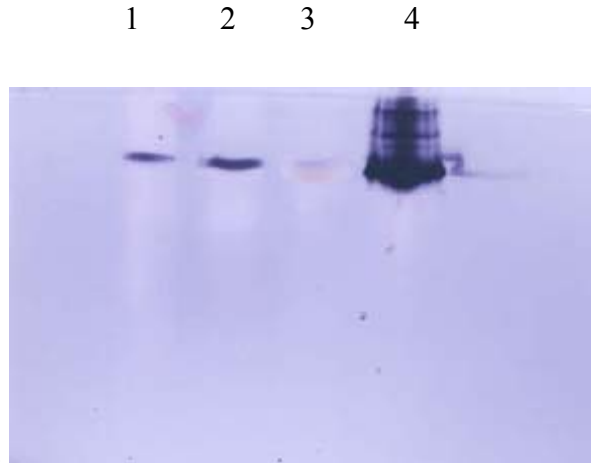


Figure 3. XDH activity in two peaks of endogenous XDH in *P. aeruginosa*. Proteins (10 μ g) were applied on 7.5% native gel-electrophoresis and stained with xanthine-NBT activity stain. 1) Endogenous XDH in *P. aeruginosa* with the imidazole concentration at 35mM 2) Endogenous XDH in *P. aeruginosa* with the imidazole concentration at 50mM 3) Separated Glu758Gln *C. acidovorans* XDH 4) WT *C. acidovorans* XDH

Table 2 summarizes purification steps and enzyme yields for the mutant preparations with respect to the WT enzyme. The yield for Glu758Gln is much lower (only 1.28 mg of pure enzyme per liter of culture), compared with the amount obtainable from Glu277Gln and wild-type enzyme^[87]. Specific activities measured at each step of the purification shows a pronounced difference between WT and mutant form of XDH. Glu758Gln XDH, is only 0.002% active with respect to wild-type XDH. Both mutants exhibit positive cross-reactivity against *C. acidovorans* XDH antisera as shown by the

Western Blot (Figure 4A). SDS-PAGE (Figure 4B) shows that Glu758Gln obtained is in high level of purity. The purity is also suggested by the the A_{280}/A_{450} ratio exhibited by the mutant.

Table 2. Comparison of the purification steps for recombinant WT ^[15] and Glu758Gln *C. acidovorans* XDH. ^a

Purification step	Total protein (mg)	Total activity (U)	Specific activity (U/mg)	Yield (%)
WT				
Crude extract	535.5 ^b	2835	5.29	100.0
DE-52 column	52.0 ^b	1774	34.11	62.6
Ni-NTA column	11.9 ^c	1014	80.0	35.8
Glu758Gln				
Crude extract	880.4 ^b	0.5062	0.00057	100
DE-52 column	44.8 ^b	0.08925	0.002	17.6
Ni-NTA column	1.28 ^c	0.0011	0.0009	0.2

^aRecalculated for 1 L of culture.

^bBased of Biuret assay.

^cBased on A_{450} and $\epsilon_{450} = 37,000 \text{ M}^{-1}\text{cm}^{-1}$.

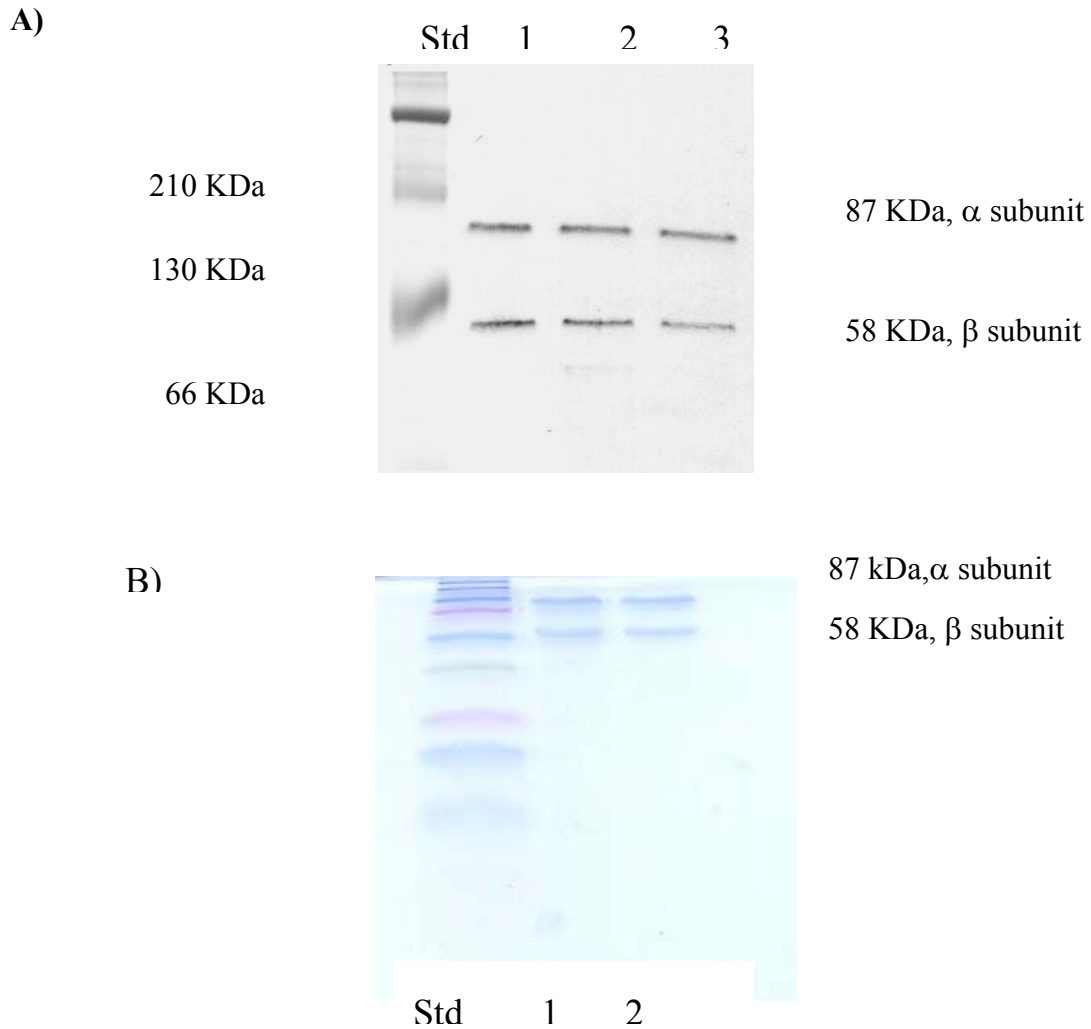


Figure 4. Characterization of Glu758Gln. A) Western blot against *C. acidovorans* XDH antisera, and B) SDS-PAGE. 1) WT, 2) Glu 277 Gln and 3) Glu758Gln.

3.3.2 Characterization of recombinant Glu758Gln from *P. aeruginosa* PAO1-LAC

3.3.2.1 Spectral properties of recombinant Glu758Gln XDH

UV-Vis spectra of Glu758Gln look remarkably similar to that of the WT enzyme (Figure 5) ^[15], featuring the characteristic absorption bands of the flavin (450 and 370 nm) and of the 2 [2Fe-2S] clusters (467 and 420 nm).

Circular Dichroism spectra of resting Glu758Gln (Figure 6) show the intense positive dichroic bands typical of the oxidized [2Fe-2S] clusters at 470 and 430 nm. Bleaching of the chromophores is found upon reduction with dithionite.

EPR spectra show the intactness of [2Fe-2S] clusters in Glu758 mutant XDH.

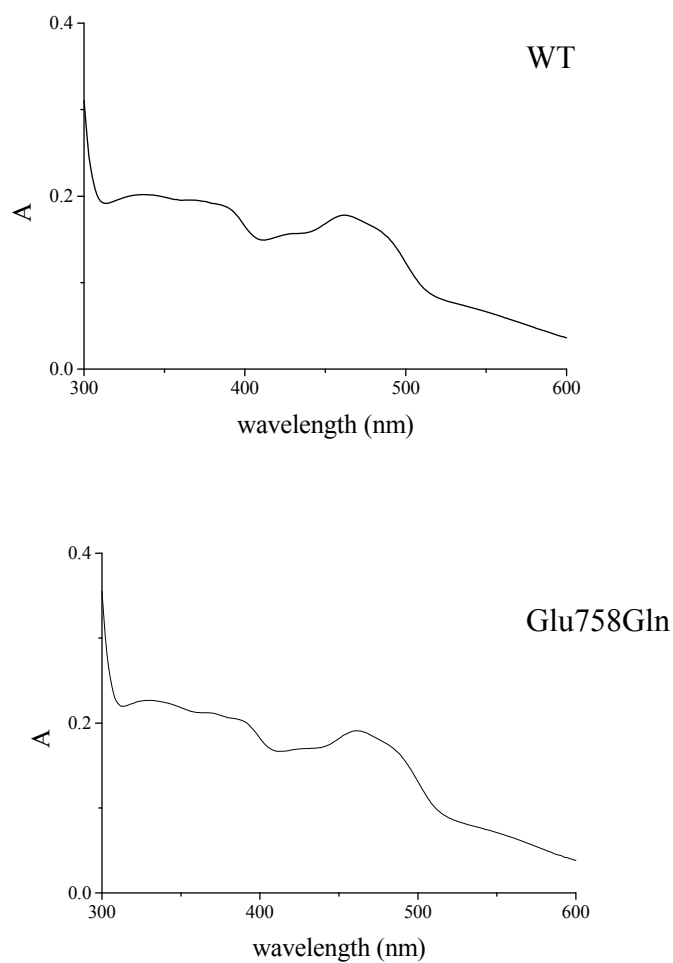


Figure 5. UV-Vis spectra of WT (top, ~4 μ M) and Glu758Gln XDH (bottom, ~5 μ M). 25°C.

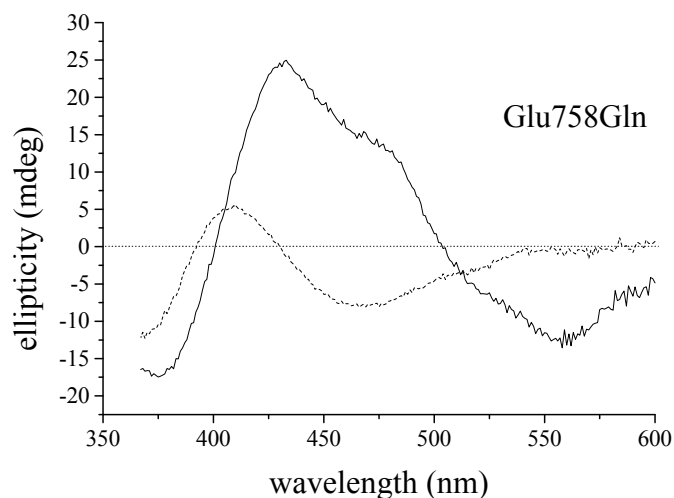


Figure 6. Circular Dichroism spectra of Glu758Gln XDH (15 μ M). Solid traces refer to resting enzymes; dashed traces refer to dithionite reduced enzymes. Spectra where recorded anaerobically at 25 $^{\circ}$ C.

3.3.2.2 Chemical properties and kinetic parameters of recombinant Glu758Gln at pH 7.8

Table 3 summarizes cofactor analyses and kinetic parameters measured at pH 7.8 for wild-type and Glu758Gln *C. acidovorans* XDH. Practically all the Mo found in Glu758Gln is functional. The presence of \sim 4 Fe per flavin is demonstrated by metal analysis data and confirmed by the previously discussed UV-Vis and CD spectroscopic properties of Glu758Gln.

Specific activities and turnover numbers recalculated per amount of functional enzyme (Mo=S) also reflect the huge catalytic difference between WT and the mutant (Table 3). The $k_{cat}/\text{Mo}=\text{S}$ of Glu758Gln is 0.0062 s^{-1} , 0.002% of wild-type enzyme.

However, K_m for xanthine of Glu758Gln is only 30% of the wild-type XDH. K_m for NAD^+ for the mutant is found to be about half of that exhibited by the wild-type enzyme.

Table 3. Comparison of the properties of pure recombinant WT ^[15] and Glu758Gln *C. acidovorans* XDH, steady state kinetic parameters were measured at pH 7.8.

Property	WT	Glu758Gln
Mo/flavin	0.89	0.48
Mo=S^a	0.86	0.47
Fe/flavin	3.93	4.58
Specific activity (U/flavin ratio)	80.0	0.0018
Spec. Act. /Mo=S (U/Mo=S)	93	0.0038
k_{cat} (sec⁻¹)	220 ± 7	0.0029 ± 0.000079
k_{cat}/Mo=S (sec⁻¹)	255 ± 8	0.0062 ± 0.00016
K_m xanthine (μM)	120 ± 5	35 ± 4.7
K_m NAD^+ (μM)	81 ± 14	41 ± 8
A₂₈₀/A₄₅₀	4.9	7.5

^aThe amount of functional Mo=S^[14] was determined by the method reported by Sorbo.
[79]

3.4 Discussion

As previously observed for the WT enzyme ^[15], the pUCP-Nde/*P. aeruginosa* expression system allows expression of Glu758Gln *C. acidovorans* XDH in high yield and with high levels incorporation of functional Mo=S.

The expressed mutant enzyme was His-tagged at the N-terminus of the β subunit to allow purification with metal affinity chromatography. The endogenous XDH in *P. aeruginosa* shows activity after Ni-NTA column, showing the endogenous XDH can also

bind to the Ni-NTA column. This might occur because there are some imidazole clusters present in the endogenous XDH of *P. aeruginosa*. Endogenous XDH in *P. aeruginosa* is 0.0273 U/L, and it is 0.0027% of the total units as that of the WT enzyme. Therefore, for WT enzyme and the Glu277Gln mutant with high activity ^[87], the activity that the endogenous XDH in *P. aeruginosa* attributes is negligible. However, the activity of the Glu758Gln mutant is rather low and is only about 4% of the total units as that of the endogenous XDH in *P. aeruginosa*, and the presence of endogenous XDH can definitely interfere with the observed kinetic behavior of the expressed enzyme. Therefore, separating the endogenous XDH from the expressed mutant XDH is necessary for the investigation of Glu758Gln recombinant XDH.

Recombinant mutant forms of the enzyme exhibit UV-Vis and CD spectral properties very similar to the wild-type enzyme. Determination of the cyanolyzable S in Glu758Gln demonstrates that most of the Mo in Glu758Gln is in the sulfurated active form.

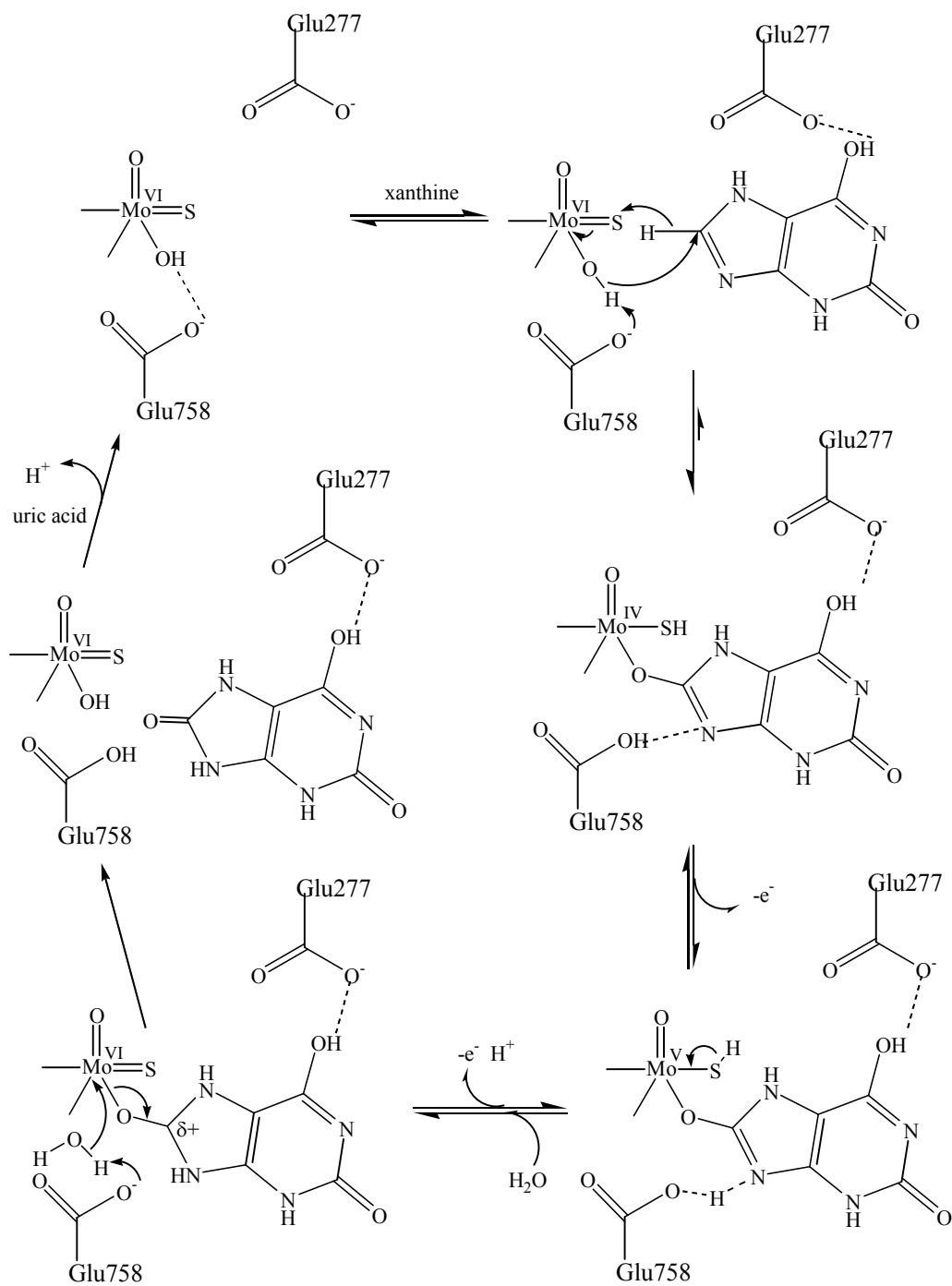
Kinetic characterization of Glu758Gln *C. acidovorans* XDH at pH 7.8 reveals that Glu758Gln $k_{cat}/\text{Mo}=\text{S}$ is 0.0062 s⁻¹ (0.002% of WT). Furthermore, specific activities and turnover numbers of the mutant show the greatest difference to those measured for the wild-type enzyme. Specific activities and k_{cat} values recalculated for amount of functional molybdenum (Mo=S) reflect a difference of about 5 orders of magnitude for Glu758Gln, and the difference in catalytic activity translates in a $\Delta(\Delta G)$ for the reaction that we

determined to be ~6.4 Kcal/mol for Glu758Gln with respect to the WT enzyme. This considerable gap in ΔG documents the crucial role of the glutamate residue plays in promoting the oxidation of the substrate. Similar results were previously obtained for *R. capsulatus* XDH mutants ^[86]. However, the mutation of Glu730 (structural equivalent of Glu758 in *C. acidovorans* XDH) to Gln led to an enzyme preparation with non-detectable activity in *R. capsulatus* XDH. The high level expression system allowed us to characterize *C. acidovorans* Glu758Gln mutant with detectable activity.

On the basis of our experimental evidence for Glu758Gln and the study on the Glu277Gln XDH in our lab ^[87], we propose the catalytic mechanism of *C. acidovorans* XDH to proceed as exemplified in Scheme 1. Glu758, acting as a general base, deprotonates the Mo-OH group facilitating its nucleophilic attack on the C8 of xanthine, kept in position by an hydrogen bond interaction with Glu277, and H⁻ transfer to the terminal sulfur. The proposal of Mo-OH deprotonation by Glu758 is based on the assumption that the pK_a of the Mo-hydroxyl group is of magnitude comparable to that of the glutamate ^[87]. This hypothesis is supported by previous data published for sulfite oxidase ^[88] and milk xanthine oxidase ^[24] that shows an EPR detectable Mo(V)-proton coupling at acidic pH values that disappears at basic pH values. pK_a values of 8.2 and 10 were assigned to a Mo(V)-OH species in SO and XO, respectively. Reduction at the Mo results in formation of a Mo(IV) intermediate that immediately loses one electron through [2Fe-2S] I, give rise at the Mo(V) adduct that produces the characteristic “very-rapid”

EPR feature. The protonated Glu758 can form a hydrogen bond to the N9 of xanthine, similarly to that detected in the crystal structure bovine milk XDH between Glu1261 and the N1 of 4-[5-Pyridin-4-yl-1H-[1,2,4]triazol-3-yl]pyridine-2-carbonitrile (FYX-051) ^[85]. Finally, further reduction to Mo (VI) results in release of uric acid, and product release is facilitated by the Glu758-assisted nucleophilic attack of a new water molecule.

In conclusion, with the aid of our high-level expression system pUCP-Nde/ *P. aeruginosa*, we expressed and characterized Glu758Gln active site mutant of *C. acidovorans* XDH. The low activity of the expressed mutant compared with wild-type and other mutant XDH made it necessary to remove any endogenous XDH in *P. aeruginosa*, and also 0.002% of turnover numbers compared with the wild-type XDH showed the essential roles that Glu758 in *C. acidovorans* plays in the catalytic mechanism. Therefore combining our discovery with the previous results ^[87], we presented a mechanism that proposes a double role for the catalytic essential Glu758. In our proposed mechanism, Glu758 not only assists the nucleophilic attack of Mo-OH to xanthine C8, but has also an active role in helping the release of the product, which is very important for the whole catalytic procedure.



Scheme 1 Proposed mechanism for the reductive half reaction of *C. acidovorans* XDH.

Chapter 4

General Summary

The dissertation is the result of work accomplished under the supervision of Dr. Dale E. Edmondson for the studies on *C. acidovorans* xanthine dehydrogenase, a molybdenum hydroxylase.

The characterization of *C. acidovorans* xanthine dehydrogenase from the Edmondson laboratory demonstrated similarities in the characteristics and spectral properties with the eukaryotic enzymes. The first part of the dissertation describes the characterization for *Comamonas acidovorans* xanthine dehydrogenase as a model for eukaryotic xanthine oxidoreductase which is important in many aspects of the metabolisms and related to our health by performing as the terminal enzymes in purine degradation. Aldehyde oxidase, which is also an important enzyme in plants and mammals, is in the same group of molybdenum hydroxylase as xanthine dehydrogenase, and shares many similarities with dehydrogenase.

The Chapter 1 summarizes the previous study on xanthine dehydrogenase and aldehyde oxidase, including their functions, contents and biosynthesis of cofactors, reactions, spectroscopic studies, kinetics studies, mechanisms and expression systems. The mechanism studies on xanthine dehydrogenase and the correlations between these

two enzymes provides us insights for the mechanisms for both enzymes, enabling the design more effective inhibitors to treat related diseases.

Chapter 2 describes the engineering of the *C. acidovorans* xanthine dehydrogenase to a molybdo-enzyme with aldehyde dehydrogenase functional properties. Through the comparison of the similarities and difference between XDH and AO in the general structure, cofactor contents, gene sequences and substrate specificity, the Arg355 in the active site of *C. acidovorans* xanthine dehydrogenase is chosen as a predicted point to convert the function of XDH to aldehyde dehydrogenase with the benefit of computational analysis. To realize the function conversion between XDH and ADH, the Arg355 was mutated to Met, the residue that is present in the corresponding position to Arg355 in aldehyde oxidase, by site-directed mutagenesis. The mutant enzyme Arg355Met *C. acidovorans* XDH shows an identical Uv-vis and circular dichroism spectroscopic properties and SDS-PAGE, western blot analysis results as the wild-type XDH, indicating the integrity of flavin cofactors, [Fe-S] clusters and the subunits in the mutant enzyme. Kinetics analysis of Arg355Met XDH for xanthine, hypoxanthine, purine, benzaldehyde, phenanthridine, N-methylnicotinamide was performed. The mutant shows decreases by 99.7% and 96.4% in the catalytic activities for xanthine and hypoxanthine, respectively, indicating the importance of Arg355 in the hydroxylation of xanthine in XDH. An increase in the activity with phenanthridine and benzaldehyde was observed. The increase in the activity for the substrates of aldehyde oxidase revealed the

function conversion from XDH to AO by a single amino acid change. The product of phenanthridine oxidation by Arg355Met XDH was proven to be 6-phenanthridone, the same product as oxidized by aldehyde oxidase, utilizing UV-vis spectroscopy and thin layer chromatography. The kinetic analysis of the reactions between phenanthridine and NAD^+ catalyzed by Arg355M35 shows parallel line behaviors, which is the same as xanthine hydroxylation by the wild-type XDH. The inhibitory effect of phenanthridine on the wild-type XDH shows a competitive inhibition on hydroxylation of xanthine with the inhibition constant about 11 times of the K_m of phenanthridine for the mutant enzyme as a substrate. The results suggest aldehyde oxidase is probably following a similar mechanism and catalytic pathways for aldehyde oxidation as in XDH.

Chapter 3 investigates the catalytic role of Glu758 in the active site of the XDH by studying the mutant enzyme Glu758Gln XDH. Glu758 is universally conserved, and it was shown to be important for the enzyme activity by the previous studies. The Glu758Gln XDH was purified after expression by Dr. Trani. An imidazole gradient was used for elution from Ni-NTA column during purification to separate the endogenous XDH in *P. aeruginosa* from the expressed mutant enzyme, because the presence of endogenous XDH will interfere with the kinetic behavior of the expressed enzyme that exhibits a very low catalytic activity. The recombinant mutant enzyme exhibits UV-Vis and CD spectral properties very similar to the wild-type XDH, and kinetic characterization of the Glu758Gln XDH at pH 7.8 reveals only 0.002% of turnover

number of the wild-type XDH. The result shows the importance of Glu758 in the catalytic mechanism of xanthine hydroxylation. Combined with previous results from our lab, a catalytic mechanism was proposed with Glu758 as a general base to initiate the reaction by deprotonates the Mo-OH group. The protonated form of Glu758 is also proposed in the mechanism to form a hydrogen bond to the N9 of xanthine.

References:

- [1] R. Hille, *Archives of Biochemistry and Biophysics* **2005**, *433*, 107.
- [2] K. N. Murray, J. G. Watson, S. Chaykin, *Journal of Biological Chemistry* **1966**, *241*, 4798.
- [3] A. P. Tisler, Andreas; Honey, John D'Arcy; Bull, Shelley B.; Rosivall, Laszlo; Logan, Alexander G., *Nephrology, Dialysis, Transplantation* **2002**, *17*, 253.
- [4] H. A. R. Simmonds, S., and Nishino, T., *The metabolic and molecular bases of inherited disease*, Vol. 2, 7th ed., McGrawHill, New York, **1995**.
- [5] J. L. a. W. Johnson, S. K., **1989**, pp. 1463.
- [6] Y. Kuwabara, Nishino, T., Okamoto, K., Matsumura, T., Eger, B.T., Pai, E. F., and Nishino, T., *PNAS* **2003**, *100*, 8170.
- [7] V. Massey, Brumby, P.E. and Komai, H., *Journal of Biological Chemistry* **1969**, *244*, 1682.
- [8] R. Hille, *Chemical Reviews* **1996**, *96*, 2757.
- [9] J. L. Johnson, Chaudhury, M, Rajagopalan, K.V., , *Biofactors* **1991**, *3*, 103.
- [10] Q. Xiang, Edmondson, D. E., *Biochemistry* **1996**, 5441.
- [11] S. Leimkuhler, Kern, M., Solomon, P.S., McEwan, A.G., Schwarz, G., Mendel, R.R. and Klipp, W., *Mol. Microbiol.* **1998**, *27*, 853.
- [12] M. S. Neumann, M.;Junemann, N.; Stocklein, W.; Leimkuhler, S., *J. Biol. Chem.* **2006**, *281*, 15701.
- [13] C. Enroth, Eger, B. T., Okamoto, K., Nishino, T., Nishino, T., Pai, E. F., *PNAS* **2000**, *97*, 10723.
- [14] V. Massey, and Edmondson, D. E., *The Journal of Biological Chemistry* **1970**, 6595.
- [15] N. V. Ivanov, Trani, M., and Edmondson, D.E., *Protein Expression and Purification* **2004**, *72*.
- [16] M. M. Wuebbens, K. V. Rajagopalan, *Journal of Biological Chemistry* **1993**, *268*, 13493.
- [17] J. A. S.-A. G. Schwarz, S. Wolf, H.J. Lee, I.M. Adam, H.J. Grone, H. Schwegler, J.O. Sass, T. Otte, P. Hanzelmann, R.R. Mendel, W. Engel, J. Reiss, *Human Mol. Genet.* **2003**, *13*, 1249.
- [18] S. K. Leimkuhler, W., *Journal of bacteriology* **1999**, *181*, 2745.
- [19] N. V. Ivanov, Hubalek, F. Trani, M. and Edmondson, D.E., *European Journal of Biochemistry* **2003**, *270*, 4744.
- [20] U. Muhlenhoff, Lill, R., *Biochimica Biophysica Acta* **2000**, 370.
- [21] M. Nakamura, Saeki, K. and Takahashi, Y., *Journal of Biochemistry (Tokyo)* **1999**, *126*, 10.
- [22] A. Bacher, Eberhardt, S., Fischer, M., Kis, K. and Richter, G., *Annual Reviews of Nutrition* **2000**, *20*, 153.
- [23] D. Edmondson, Ballou, D., Van Heuvelen, A., Palmer, G. and Massey, V., *Journal of Biological Chemistry* **1973**, *248*, 6135.
- [24] S. T. Gutteridge, S.J.; Bray, R.C., *Biochem. J.* **1978**, 887.
- [25] D. Edmondson, Massey, V., Palmer, G., Beacham, L.M., 3rd and Elion, G.B., *Journal of Biological Chemistry* **1972**, *247*, 1597.
- [26] W. F. Cleere, Coughlan, M.P., *Comp. Biochem. Physiol. B* **1975**, 311.
- [27] D. G. Priest, Fisher, J.R., *Archives Biochemistry Biophysics* **1971**, *146*, 391.
- [28] K. V. H. Rajagopalan, P., *Journal of Biological Chemistry* **1967**, *242*, 4097.
- [29] Q. Xiang, Emory University **1996**.

- [30] J. Hunt, Massey, V., *Journal of Biological Chemistry* **1992**, 267, 21479.
- [31] L. M. Schopfer, Massey, V. and Nishino, T., *Journal of Biological Chemistry* **1988**, 263, 13528.
- [32] J. H. Kim, Ryan, M. G., Knaut, H. and Hille, R., *Journal of Biological Chemistry* **1996**, 271, 6771.
- [33] S. C. D'Ardenne, Edmondson, D.E., *Biochemistry* **1990**, 9046.
- [34] R. M. Hille, V., *Journal of Biological Chemistry* **1981**, 256, 9090.
- [35] A. G. Porras, Olson, J.S. and Palmer, G., *Journal of Biological Chemistry* **1981**, 256, 9096.
- [36] T. Nishino, Nishino, T., Schopfer, L.M. and Massey, V., *Journal of Biological Chemistry* **1989**, 264, 2518.
- [37] M. C. Walker, Hazzard, J.T., Tollin, G. and Edmondson, D.E., *Biochemistry* **1991**, 5912.
- [38] R. Hille, *Biochemistry* **1991**, 8522.
- [39] R. Hille, Anderson, R.F., *Journal of Biological Chemistry* **1991**, 266, 5608.
- [40] B. D. Howes, Bray, R.C., Richards, R.L., Turner, N.A., Bennett, B. and Lowe, D.J., *Biochemistry* **1996**, 1432.
- [41] R. J. Greenwood, G. L. Wilson, J. R. Pilbrow, A. G. Wedd, *Journal of the American Chemical Society* **1993**, 115, 5385.
- [42] M. Xia, Dempksi, R., and Hille, R., *Journal of Biological Chemistry* **1999**, 274, 3323.
- [43] J. H. Kim, R. Hille, *Journal of Biological Chemistry* **1993**, 268, 44.
- [44] W. A. a. H. Oertling, R., *Journal of Biological Chemistry* **1990**, 265, 17446.
- [45] R. Hille, George, G.N., Eidsness, M.K. and Cramer, S.P., *Inorganic Chemistry* **1989**, 4018.
- [46] T. Nishino, Saito, Y., Amaya, S., Kawamoto, S., Ikemi, Y. Nishino, T., in *Flavins and Flavoproteins, Vol. 1994* (Ed.: K. Yagi), de Gruyter, Berlin, **1993**, pp. 711.
- [47] B. Adams, Smith, A. T., Doyle, R.C., Bray, R. C., Ryan, M., Harrison, A.J., Wolstenholme, A.J., Romao, M.J., Huber, R., Demais, S., Scazzocchio, C., *Biochemical Society Transactions* **1997**, 25, 520S.
- [48] W. A. Doyle, Burke, J.F., Chovnick, A., Dutton, F.L., Russell, J.R., Whittle, J.R. and Bray, R.C., *Biochemical Society Transactions* **1996**, 24, 31S.
- [49] R. R. Mendel, F. Bittner, *Biochimica Et Biophysica Acta-Molecular Cell Research* **2006**, 1763, 621.
- [50] R. R. M. Günter Schwarz, *Annual Review of Plant Biology* **2006**, 57, 623.
- [51] M. K. M. Terao, G. Saltini, S. Demontis, M. Marini, M. Salmona, E. Garattini,, *Journal of Biological Chemistry* **2000**, 275, 30690.
- [52] M. K. M. Terao, M. Marini, M.A. Vanoni, G. Saltini, V. Bonetto, A. Bastone, C. Federico, S. Saccone, R. Fanelli, M. Salmona, E., Garattini, *Journal of Biological Chemistry* **2001**, 276, 46347.
- [53] S. Shaw, E. Jayatilleke, *Biochemical Journal* **1990**, 268, 579.
- [54] R. R. Mendel, Hänsch, R., *Journal of Experimental Botany* **2002**, 53, 1689.
- [55] H. K. M. Seo, S. Akaba, T. Komano, T. Oritani, Y. Kamiya, T., Koshiba, *Plant journal* **2000**, 2000, 481.
- [56] R. Huber, P. Hof, R. O. Duarte, J. J. G. Moura, I. Moura, M. Y. Liu, J. LeGall, R. Hille, M. Archer, M. J. Romao, *Proceedings of the National Academy of Sciences of the United States of America* **1996**, 93, 8846.
- [57] L. P. E. a. L. A. L. Adonis Skandalis, *chemistry & Biology* **1997**, 4, 10.

- [58] K. M. a. H. O. Yosuke Terao, *Chemistry Communication* **2006**, 3.
- [59] K. L. M. a. R. J. Kazlauskas, *TRENDS in biotechnology* **2005**, 23, 7.
- [60] C. H. Yvonne N. Fondufe-Mittendorf, Wilfried Kramer and Hans-Joachim Fritz, *Nucleic Acids Research* **2002**, 30, 8.
- [61] R. M. Enrico GARATTINI, Maria João ROMÃO, Richard WIGHT and Mineko TERAO, *Biochemical Journal* **2003**, 372, 18.
- [62] C. A. G. Temple, T. N.; Rajagopalan, K. V. , *Archives of Biochemistry and Biophysics* **2000**, 383, 281.
- [63] M. L. Calzi, C. Raviolo, E. Ghibaudi, L. DeGioia, M. Salmona, G. Cazzaniga, M. Kurosaki, M. Terao, E. Garattini, *Journal of Biological Chemistry* **1995**, 270, 31037.
- [64] F. B. Ralf R. Mendel, *Biochimica et Biophysica Acta* **2006**, 1763, 621.
- [65] R. T. F. Rodriguez-Trelles, F.J. Ayala,, *Proc. Natl. Acad. Sci* **2003**, 100, 13413.
- [66] T. Ghafourian, M. R. Rashidi, *Chemical & Pharmaceutical Bulletin* **2001**, 49, 1066.
- [67] Krenitsk.Ta, G. B. Elion, Hitching.Gh, S. M. Neil, *Archives of Biochemistry and Biophysics* **1972**, 150, 585.
- [68] C. Beedham, *Molybdenum Hydroxylases: Biological Distribution and Substrate- Inhibitor Specificity*. *Progress in Medicinal Chemistry*, Elsevier Science Publishers, B.V., London, **1987**.
- [69] Krenitsk.T.A, G. B. Elion, Hitching.Gh, S. M. Neil, *Archives of Biochemistry and Biophysics* **1972**, 150, 585.
- [70] K. R. K. Rhonda A. Torres, Daniel R. Mcmasters, Christine M. Fandozzi, Jeffrey P. Jones, *Journal of Medicinal Chemistry* **2007**, 50, 4642.
- [71] J. J. Truglio, K. Theis, S. Leimkuhler, R. Rappa, K. V. Rajagopalan, C. Kisker, *Structure* **2002**, 10, 115.
- [72] A. Glatigny, P. Hof, M. J. Romao, R. Huber, C. Scazzocchio, *Journal of Molecular Biology* **1998**, 278, 431.
- [73] E. G. a. H. K. MITCHELL, *Genetics* **1959**, 44, 153.
- [74] N. V. Ivanov, Emory University (Atlanta), **2002**.
- [75] C. N. Cronin, McIntire, W.S., *Protein Expression and Purification* **1999**, 272, 112.
- [76] C. N. Cronin, McIntire, W.S., *Protein Expression and Purification* **2000**, 19, 74.
- [77] A. G. Gornall, Bardawill, C.J., Davd, M.M., *Journal of Biological Chemistry* **1949**, 177, 751.
- [78] U. K. Laemmli, *Nature* **1970**, 227, 680.
- [79] B. Sorbo, *Biochim. Biophys. Acta* **1957**, 324.
- [80] S. M. Taylor, C. Stubblebeedham, J. G. P. Stell, *Biochemical Journal* **1984**, 220, 67.
- [81] Y. Yamaguchi, T. Matsumura, K. Ichida, K. Okamoto, T. Nishino, *Journal of Biochemistry* **2007**, 141, 513.
- [82] B. C., *Enzymes systems that Meabolize Drugs and Other Xenobiotics*, Ioannides C., John Wiley & Sons, New York, **2002**.
- [83] G. I. Panoutsopoulos, C. Beedham, *Acta Biochimica Polonica* **2004**, 51, 649.
- [84] R. C. G. Bray, S., *Biochemistry* **1982**, 21.
- [85] K. Okamoto, Matsumoto, K., Hille, R., Eger, B. T., Pai, E. F., Nishino, T. , *Proceedings of the National Academy of Sciences of the United States of America* **2004**, 101, 7931.

- [86] S. Leimkuhler, Stockert, A.L., Igarashi, K., Nishino, T., and Hille, R., *Journal of Biological Chemistry* **2004**, 279, 40437.
- [87] M. Trani, Emory University (Atlanta), **2006**.
- [88] H. J. Cohen, Fridovich, I., and Rajagopalan K.V., *Journal of Biological Chemistry* **1971**, 246, 374.